SEMMELWEIS EGYETEM

DOKTORI ISKOLA

Ph.D. értekezések

2873.

PAJTÓK CSENGE

Krónikus betegségek gyermekkori prevenciója
című program

Programvezető: Dr. Szabó Attila, egyetemi tanár

Témavezetők: Dr. Pap Domonkos, tudományos főmunkatárs

EFFECT OF HIGH SALT DIET ON DERMAL TISSUE REMODELING

PhD thesis

Csenge Pajtók, MD

Károly Rácz Clinical Medicine Doctoral School

Semmelweis University

Supervisor: Domonkos Pap, Ph.D

Official reviewers: Nóra Ledó, MD, Ph.D

Noémi Sándor, Ph.D

Head of the Complex Examination Committee: András Szabó, MD, D.Sc

Members of the Complex Examination Committee: Tamás Szabó, Ph.D

András Tislér, D.Sc

Budapest

2023

Table of Contents

List of Abbreviations

ACTA2: α-SMA: alpha-smooth muscle actin

ACTB: beta-actin

bp: base pair

BrdU: bromodeoxyuridine

COL1A1: collagen-1a1

COX-2: cyclooxygenase-2

DF: dermal fibroblast

ECM: extracellular matrix

EGF: epidermal growth factor

F: forward

FN: fibronectin

GAG: glycosaminoglycan

GAPDH: glyceraldehyde 3-phosphate dehydrogenase

HSD: high salt diet

IBD: inflammatory bowel diseases

IL: interleukin

IMQ: imiquimod

LDH: lactate dehydrogenase

MMP: matrix metalloproteinase

MRI: magnetic resonance imaging

MTT: thiazolyl blue tetrazolium bromide

NLRP3: NLR family pyrin domain containing 3

NSD: normal salt diet

OÉTI: National Institute of Food and Nutrition

PBMC: peripheral blood mononuclear cell

PCR: polymerase chain reaction

PDGF-B: platelet-derived growth factor

PGE2: prostaglandin E2

R: reverse

Ta: annealing temperature

TAS: transient agarose spot

TGF-ß: transforming growth factor-beta

Th: T helper

TLR7: toll-like receptor 7

TNF-α: tumor necrosis factor-alpha

TonEBP: osmosensitive transcription factor

VCL: vinculin

VEGF-C: vascular endothelial growth factor C

VIM: vimentin

WHO: World Health Organization

1. Introduction

1.1 Salt consumption in modern societies

The spread of processed foods, rapid urbanization, and changing lifestyles have radically transformed the eating habits of Western societies. Processed foods are becoming more accessible and affordable, however they contain much more salt (NaCl) than foods consumed in their natural state [1]. NaCl is the primary source of sodium (Na^+) for our body. Na^+ is known to be essential for nerve and muscle function and is involved in regulating the body's fluid balance [2]. However, according to the classic view excessive salt intake is associated with increased risk of several diseases of civilization, including hypertension, heart disease, or stroke.[3, 4]. The World Health Organization (WHO) recommends the reduction of salt intake as a population-level intervention to reduce cardiovascular disease and mortality [5]. Indeed, the recommended average salt consumption in the general population is 5 g/day (equivalent to 2 g/day of sodium), however the salt intake of modern societies far exceeds the direction of WHO in almost every country in the world (Fig 1) [5, 6]. According to the study conducted by the Hungarian National Institute of Food and Nutrition (OÉTI), Hungarian women consume up to 2.5 times, while men consume at least 3.5 times more salt than recommended [7].

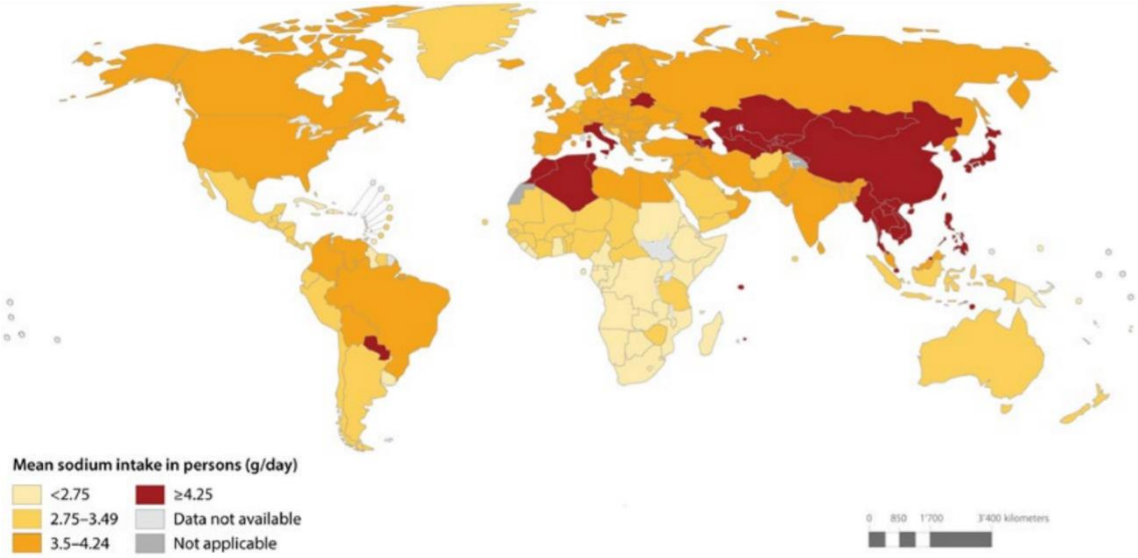

Figure 1. Estimated mean sodium intake in persons aged 20 years and over [8].

1.2 Renal regulation of Na^+ excretion

Sodium homeostasis is classically considered to be regulated by the kidneys. Several hormones are involved in the regulation of Na^+ and water homeostasis, including the

renin-angiotensin-aldosterone system (RAAS), atrial natriuretic peptide (ANP), and vasopressin [9]. Increased salt intake inhibits RAAS, thereby increasing natriuresis, while low salt intake stimulates renin release [9]. Renin splits angiotensinogen to produce angiotensin I, which is further converted to angiotensin II, a potent blood pressure-inducing peptide hormone. In this way, renin indirectly raises blood pressure. The main function of ANP is to decrease the volume of expanded extracellular fluid (ECF) by increasing renal sodium excretion [10]. The increased plasma Na^+ concentrations stimulate the release of vasopressin, which in turn promotes water reabsorption [11]. Besides the hormonal effect, a major mediator of renal sodium excretion is arterial pressure. Salt sensitivity of arterial blood pressure is a physiological property by which the blood pressure in a proportion of the population exhibits changes in parallel with changes in salt intake [12]. Indeed, dietary salt loading increases blood pressure of salt-sensitive humans, resulting in increased Na^+ excretion [13]. On average, an adult person filters more than 25 000 mmol/day of sodium through the kidneys, but much of it is reabsorbed and less than 1% of the filtrate is excreted in the urine [14]. The unnecessary amount of salt is also excreted by the kidneys, however there are other mechanisms of our body that correct the imbalance of sodium homeostasis caused by excessive salt intake.

1.3 Skin – our largest Na^+ storage

For more than 100 years, direct chemical measurements have shown that the skin is a depot of sodium, chloride and water, however, the exact relevance of dermal electrolytes and the molecular mechanism of their storage remained unknown [15-18]. Several recent investigations, including chemical analysis in experimental animal models as well as quantitative ^{23}Na-MRI observations on humans demonstrated that sodium can be stored in the skin without commensurate water retention [19-25].

The skin is our largest organ providing the mechanical, physical, chemical, microbiological and immunological protection, as well as the balance of heat and water homeosthasis. The skin accounts for 6% of body weight and a significant component of the interstitium [26, 27]. The harmonious relationship between the body and the outside environment requires the intact structure and function of the skin. The two tissue layers of the skin are the epidermis, which is the outer layer of skin consisting of non-layered epithelial cells, and the dermis, which contains mainly connective tissue [27]. The

epidermis acts as a physical barrier against water loss and microorganisms, while the dermis is relatively acellular, consisting of fibroblasts, nerves, immune cells, lymphatics, and blood vessels in an extracellular matrix (ECM) composed mostly of collagen and glycosaminoglycans (GAG) [27, 28]. GAGs are high molecular weight, long-chained, polyanionic, polysaccharide molecules. There are six key types of GAGs; the sulfated (1) chondroitin sulfate, (2) dermatan sulfate, (3) heparan sulfate, (4) heparin, (5) keratan sulfate and the non-sulfated (6) hyaluronic acid [29]. It has been demonstrated that GAGs play a central role in dermal Na^+ storage. Indeed, due to their high negative charge density, they can bind positively charged ions, including Na^+, resulting in an osmotically inactive dermal Na^+-store. In addition, Na^+ can be stored in a free, osmotically active form in the skin [22]. Dermal Na^+ concentration has been shown to correlate with GAG content [30]. Accordingly, based on the results of our and other research groups high salt consumption increases dermal Na^+ content as well as the amount of GAGs of the skin [22, 23, 31], while as a result of salt reduction, both Na^+ and GAG decrease [32-34] (Fig 2). Serving as a buffer against Na^+ overload, GAGs may blunt blood pressure rise by storing Na^+ [35, 36]. Correspondingly, interstitial electrolyte balance is regulated not only by the kidneys but also by extrarenal regulatory mechanisms within the skin interstitium via GAGs. Although the underlying molecular mechanisms of dermal GAG regulation are still unknown in detail, our research group recently revealed a new dermal fibroblasts (DF)- mediated regulation of GAG synthesis in the skin during salt overload [31]. Our results showed that high sodium concentration activates the cyclooxygenase-2 (COX-2)/ prostaglandin E2 (PGE2) pathway and the consequently elevated PGE2 induces GAG production. In case of excessive salt intake, the plasma Na^+ concentration has been shown to increase only briefly and slightly above the mean concentration of 140 mmol/l. In contrast, the concentration of Na^+ in the dermal interstitium can reach up to 180 mmol/l [23]. In addition, hyperosmolarity has been shown to develop in the skin of animals kept on high salt diet [21].

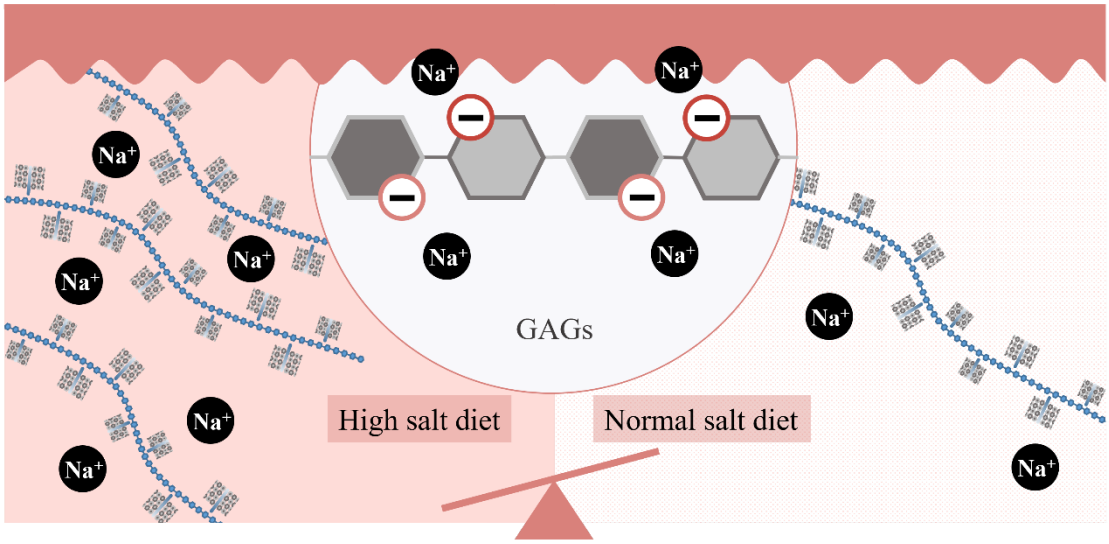

Figure 2. Sodium storage by glycosaminoglycans in skin interstitium

(Szerkesztő program: Microsoft PowerPoint)

1.4 Effect of salt intake on skin pathology

Increasing number of experimental data suggest that local sodium excess mediates pathological processes in the skin. Indeed, skin regions affected by atopic dermatitis has been shown to contain elevated sodium levels compared to non-lesion atopic and healthy skin [37]. Furthermore, there might be a correlation between increased dietary salt intake and aggravation of symptoms of psoriasis in humans [38, 39]. It has also been reported that high salt intake can delay wound closure in the skin by reducing macrophage activation [40]. Taken together, these data suggest that increased salt intake has a more complex effect on the pathological processes in the skin than previously thought, although little is known about the underlying mechanisms.

1.5 Systemic, local and immunomodulatory effects of high salt intake

It has long been proven that increased salt intake contributes to the development of hypertension, cardiovascular diseases and events [3, 4, 41, 42]. Hypertension is responsible for more than 10 million deaths a year and is one of the most modifiable risk factors for stroke, heart failure, ischemic heart disease, and chronic kidney disease [43-45]. Besides the well-known role of sodium in maintaining body fluid homeostasis and blood volume recent studies demonstrated that excessive salt intake and the consequently increased local sodium amount can induce inflammation and worsen the ongoing pathological processes in various organs [46, 47].

Indeed, studies examining the effects of excessive salt intake as well as elevated salt environments have clearly demonstrated that increased salt loading has an immunomodulatory effect on cells of both innate and adaptive immune systems. High salt loading enhances the proinflammatory function of macrophages in the lung and brain, which suggests that high salt is a potential environmental risk factor for lung and brain inflammation [48-50]. In addition, high salt condition affects various immune cell populations in the kidney and promotes renal inflammation together with the development of hypertensive renal disease [51-53]. Moreover, recent studies have demonstrated that high salt diet (HSD) leads to the accumulation of sodium in the gut and exacerbates the symptoms of inflammatory bowel diseases (IBD) [54-57].

One of the underlying mechanisms of high salt pathologies assumed to be the hypertonicity induced by Na^+ concentration exceeding the Na^+-binding-capacity of GAGs in tissues, which stimulates the osmosensitive transcription factor (TonEBP) production of invading macrophages [58]. Nuclear translocation of TonEBP leads to the transcription and secretion of vascular endothelial growth factor C (VEGF-C), stimulating lymphangiogenesis. The denser lymphatic network enhances the return of Na^+ to the circulation to eventually be removed by the kidneys, preventing the increase in blood pressure associated with salt loading.

In addition, one of the best characterized salt-related inflammatory effects is the elevated differentiation of naive T cells toward Th17 cells and their increased IL-17 production [38, 59]. Since high mannitol concentration does not alter Th17 cell differentiation, Th17 cell induction by salt loading is not osmosis-related but a specific effect [59]. The polarization of Th17 cells promoted by high sodium environment leads to the development of Th17 cell mediated autoimmune diseases by inducing tissue inflammation [38, 59, 60]. IL-17 expressed by Th17 cells induces the release of chemokines, which recruit the immune cells, such as monocytes and neutrophils to the site of inflammation. Promoting the inflammation, IL-17 acts in concert with tumor necrosis factor-α (TNF-α) and IL-1β [61, 62]. The immunoregulatory cytokine transforming growth factor-β (TGF-β) and the proinflammatory cytokines IL-1β, TNF-α, and NLRP3 have been shown to be required for Th17 cell differentiation [63-67]. On the other hand, the anti-inflammatory IL-10 signaling directly suppresses Th17 cells, and IL-

13 also negatively regulates IL-17 expression through an IL-10-dependent mechanism [68-70].

Furthermore, based on previous studies, high salt concentrations increase the expression of the aforementioned inflammatory cytokines, including IL-1β, TNF-α and NLRP3 in immune cells, while decreasing the production of anti-inflammatory IL-10 in macrophages [50, 71-74].

1.6 Imiquimod (IMQ)-induced dermatitis mouse model

The pathomechanism of dermal inflammation, tissue remodeling and the effect of various molecules, compounds and treatments on its severity is frequently investigated by the imiquimod (IMQ)-induced dermatitis mouse model. IMQ, sold under the brand name Aldara cream (5% IMQ), is an immunomodulating compound that can be used to treat genital warts, superficial basal cell carcinoma and actinic keratosis [75]. The mechanism of action of IMQ is to stimulate the innate immune system by activating toll-like receptor 7 (TLR7) and other TLR7-independent immune defences including NLRP1 inflammasome activation, which induce proinflammatory signaling pathways [76, 77]. IMQ induced acute dermatitis has become the most widely used animal model of psoriasis-like skin inflammation since it was first published in 2009 [78]. In this model, Aldara is applied to the shaved dorsal skin of mice to induce scaly skin lesions and strong inflammatory response similar to plaque-type psoriasis. Based on the immunomodulatory role of topical IMQ treatment it can also be used to model dermatitis. Aldara-induced skin inflammation has several advantages in preclinical research, including rapid and reproducible skin response and relative cost-effectiveness. Therefore, in order to investigate how the long-term dietary salt intake influences the inflammation and tissue remodeling in the skin, we used the IMQ-induced tissue dermatitis model.

1.7 Tissue remodeling

Injury associated tissue remodeling is defined as the reorganization of ECM components of a specific tissue. Tissue remodeling can be either physiological which is a part of normal healing, or pathological which is an abnormal process occurring post-injury leading to fibrosis [79, 80]. Fibrosis can be characterised by excessive scarring of a specific tissue that leads to distorted tissue architecture and ultimately organ dysfunction [80]. The patomechanism of fibrosis is similar throughout the body, regardless of the cause and the organ involved [81]. The fibrotic tissue is frequently less functional than

the original. This remodeled tissue is known as a scar. Excessive enrichment of scar tissue inhibits the regeneration of functional tissue, which may lead to a reduction or loss of function of the affected organ [82]. According to some estimates nearly 45% of all death cases in the developed world are attributed to some type of chronic fibroproliferative disease [81]. As there is currently no adequate treatment for fibroproliferative diseases, inhibition of fibrosis is a widely researched field of science. Methods that allow the accurate measurements of the functional activity of fibroblast cells, including their proliferation, ECM deposition and migration have great importance in the development of antifibrotic drugs.

Regardless of the organ involved, chronic inflammation is one of the main causes of scarring. Neutrophils and macrophages arriving at the site of injury produce high levels of proinflammatory cytokines, profibrotic growth factors, such as IL-13, TGF-β, PDGF-B (platelet derived growth factor B), EGF (epidermal growth factor) and others, which stimulate the proliferation, migration and excessive ECM production of the α-SMA (α-smooth muscle actin) -positive fibroblasts, the key effector cells of organ fibrosis [80]. Fibrosis occurs when the balance between the production and degradation is shifted toward the increased production of collagen-I and –III-rich ECM. In the proteomic turnover of ECM MMPs (matrix metalloproteinases) play a key role. MMPs are not only responsible for ECM degradation, but also for the activation of growth factors, cytokines and chemokines, considered as matrix associated proteins, modulating their activity either by direct cleavage or by releasing them from ECM bound reserves. Under normal conditions, their activity is low but increases during inflammation or remodeling processes in several diseases. Two types of MMPs, MMP-2 and MMP-9, are highly associated with decreased cell migration in addition to collagen and fibronectin degradation [83, 84].

1.8 Functions of dermal fibroblasts in wound healing

Wound healing is a complex and dynamic process of replacing damaged and missing cell structures and tissue layers. When the skin barrier that protects against the external environment is disrupted, a controlled series of biochemical events is initiated to repair the damage [85]. After platelets recruit into the open wound and deposit fibrin to stop the bleeding, immune cells arrive to remove dead tissue, angiogenesis begins and dermal fibroblasts are recruited to initiate scarring (Fig 3) [86]. DFs are the main cellular

components of the dermal scar tissue, which contribute to the development of dermal tissue remodeling through their main molecular biological and functional properties including migration due to their contractile stress fibre system, proliferation, and ECM production, which is the structural element of the scar tissue [87, 88]. Fibroblasts have an elongated spindle or star shape with numerous cytoplasmic protrusions [89]. Inactive fibroblasts have a more circular morphology compared to that of activated fibroblasts. As the main effector cells of ECM production in the skin, active fibroblasts can produce I., III. and IV. types of collagen, proteoglycans, fibronectin, laminins and GAGs [90]. In case of injury, fibroblasts migrate to the site of injury through chemotactic or mechanical stimulation, proliferate and produce ECM components in response to profibrotic cytokines and growth factors. In the reparative dermis, fibroblasts are the most prominent cell type, supporting collagen formation at the site of injury. After vigorous proliferation and ECM synthesis, ECM remodeling results in the development of a near-normal tissue architecture. In addition, activated fibroblasts express *de novo* α-SMA, develop stress fibers, and generate contractile force, exerting tension on the surrounding matrix [91]. Thereby the wound undergoes physical contraction during the wound healing process (Fig 3) [92].

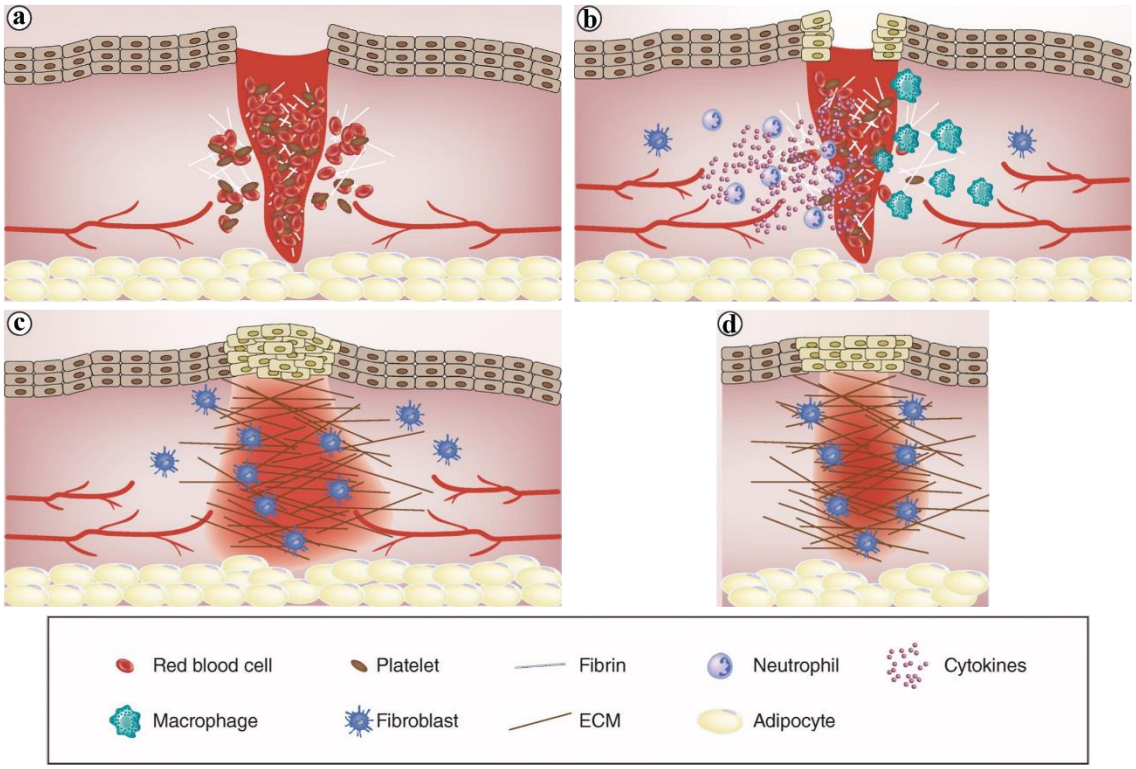

Figure 3. The pathophysiology of wound healing [86].

(**a**) In the first stage of wound healing, platelets recruit into the open wound and deposit fibrin (which serves as a pre-ECM) to stop the bleeding. (**b**) In the next stage, immune cells, including neutrophils and macrophages, recruit into the wound to remove dead tissue and debris. Angiogenesis begins at the site of injury and fibroblasts are recruited to initiate scarring. Meanwhile, on the surface, keratinocytes start to migrate to cover the wound surface of the skin. (**c**) In the remodeling phase of wound healing, keratinocytes cover the site of injury. The ECM produced by fibroblasts replaces the fibrin plug and remodels to form the final scar (**d**).

TGF-β is one of the most studied cytokine mediators of fibroblast function. TGF-β acts as a chemotactic agent and a regulator of collagen deposition [93]. TGF-β induces the activation of fibroblasts and the activated fibroblasts secrete TGF-β, creating a positive feedback loop that further exacerbates their activation and ECM production. As a growth factor, it is involved in cell structural changes and expression of α-SMA, which interacts with cellular myosin to contract and produce increased tension [94]. TGF-β induces intracellular signaling through SMAD2/3 transcription factors. Activated, i.e. phosphorylated (p)-SMAD2/3 protein regulates the expression of several profibrotic genes, including collagens, plasminogen activator inhibitor-1, various proteoglycans, integrins, and MMPs [95]. PDGF-B and EGF have also a mitogenic effect on fibroblasts [96], while the cytoskeletal component beta-actin, vimentin and vinculin increase the motility of fibroblasts [97-99], thereby playing a role in wound healing and the tissue remodeling.

1.9 Molecular processes of fibroblast migration

There are two main theories about the molecular processes underlying cell migration: cytoskeletal model and membrane flow model [100]. It is possible that both underlying processes contribute to cell movement.

The cytoskeletal model is based on the idea that certain transmembrane proteins on the cell surface connect the ECM to the part of the actin cytoskeleton adjacent to the plasma membrane, and that this part of the cytoskeleton is constantly moving backwards [101]. In this model, the rearward movement of actin filaments is balanced by assembly of the filaments at the front of the cell and depolymerization at the back of the cell [102, 103]. Due to the activity of the actin microfilaments, microtubules, and intermediate

filaments involved in cell migration, the cell becomes polarized and the shape of the cell becomes elongated [104].

In contrast, the membrane flow model describes a polarized endocytic cycle in which endocytosis occurs randomly on the cell surface while exocytosis at the front of the cell. The spatial separation of the sites of endo- and exocytosis causes plasma membrane flow from the sites of exocytosis (front of the cell) to the sites of endocytosis (back of the cell). The actin fibers formed at the front of the cell can stabilize the added membrane to form a structured protrusion or lamella.

1.10 Investigation of fibroblast migration

Since the molecular and cellular mechanisms leading to tissue fibrosis are relatively well described revealing the crucial role of fibroblast activation [79], investigating the key features of fibroblasts, including their migratory capacity [88], proliferation [80] and ECM production [90], is inevitable to identify novel therapeutic targets and develop new antifibrotic compounds. Several microplate-based assays have recently been described to investigate the different aspects of fibroblast activation. There are various well-constructed assays to examine both fibroblast proliferation (e.g. thiazolyl blue tetrazolium bromide - MTT; bromodeoxyuridine - BrdU [105]), ECM production (e.g. SiriusRed staining [106]) and migration (e.g. individual cell-tracking assay, scratch assay, transwell cell migration assay [107, 108]). The gold standard and most commonly used method for examining the migration of fibroblasts is the scratch assay (Fig 4), which is based on a graphical analysis of a cell-free area created mechanically on a cell monolayer [109]. One of the main advantages of the *in vitro* scratch assay is that it mimics the migration of cells *in vivo*. In addition, this assay is suitable for studying the regulation of cell migration by ECM-cell and cell-cell interactions, it is easy to set up, requires no special equipment, and all materials required for the assay are available in any cell culture laboratory. Although this test method is simple and cost-effective, it has significant limitations including low reproducibility or high intra-assay variability [110-113]. Besides, a relatively large amount of cells and medium is required for the assay, as it is usually performed in a 12-well tissue culture plate. Our research team recently developed an *in vitro* transient agarose spot (TAS) assay, optimised for investigating fibroblast migration in a near high-throughput manner [114]. TAS assay is an improved alternative to scratch assay, retaining its advantages and eliminating most of its limitations.

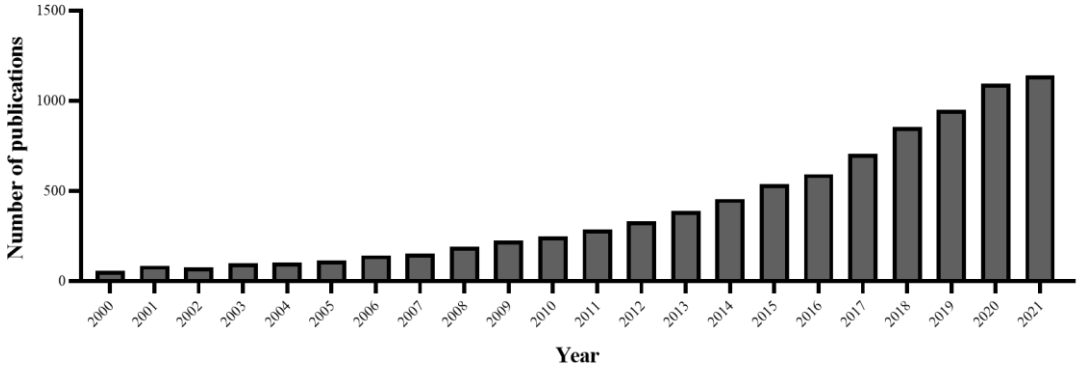

Figure 4. Use of scratch assay method in publications represented yearly [115]. According to the PubMed database, the number of publications using the scratch assay has been on an upward trend over the past 20 years.

2. Objectives

The main goal of my Ph.D. work was to better understand the effects of high salt consumption on the pathological processes of the skin, including inflammation and tissue remodeling. We also aimed to develop a new *in vitro* method that can be used to study the functional activity of fibroblast cells, the main effector cells of tissue remodeling via detection their migration capacity in response to various stimuli.

3. Methods

3.1 Animal experiments

Our experiments were approved by the Committee on the Care and Use of Laboratory Animals of the Council on Animal Care at the Semmelweis University of Budapest, Hungary (PEI/001/1731-9/2015). The experiments were performed on 7-8 weeks old male C57BL/6J mice. We kept the animals in a temperature-controlled room (22±1 °C) with alternating light and dark cycles (12/12 hours). Mice were randomly divided into four groups: normal salt diet (NSD) group; normal salt diet and imiquimod treatment (NSD IMQ) group; high salt diet (HSD) group; high salt diet and imiquimod treatment (HSD IMQ) group (n=6-8/groups) (Fig 6/a). The animals received two types of dietary regimes for 5 weeks: NSD consisting of standard rodent chow and HSD consisting of Na^+ rich rodent chow (8.0% NaCl; Ssniff Gmbh, Soest, Germany). Mice had access to food and water *ad libitum*. In our preliminary experiments, the body weights of the NSD and HSD groups were measured every 7 days for 2 weeks (n=6/groups). On the fifth week of the experiment, 62.5 mg Aldara cream (5% imiquimod; Meda AB, Solna, Sweden) was applied topically to the depilated back of mice in the NSD IMQ and HSD IMQ groups for 5 consecutive days. The local IMQ application area was 6 cm^2. Control mice in the NSD and HSD groups were treated similarly with vaseline. The general condition of the mice was monitored daily by visual examination throughout the experiment. The skinfold thickness on the backs of the mice was measured with a caliper directly before the termination of the experimental model. After the completion of the experiment, the skin was removed from the backs of the mice and snap-frozen in liquid nitrogen for further molecular biological measurements. All surgical procedures were performed under total anesthesia with intraperitoneal injection of a mixture of 100 mg/kg ketamine (Richter Gedeon, Budapest, Hungary) and 10 mg/kg xylazine (Medicus Partner, Biatorbágy, Hungary). Mice were euthanized by overdose of anesthetic solution.

3.2 Determination of skin Na^+ content

Skin samples were desiccated at 90°C for 24 hours and then digested in a mixture of 5 cm^3 Suprapur® 65% nitric acid (VWR International, Pennsylvania, USA) and 2 cm^3 Suprapur® 30% hydrogen-peroxide (VWR International) applying a TopWave microwave assisted digestion system (Analytik Jena, Jena, Germany). After this

procedure the volume of the solution was made up to 25 cm^3 with de-ionized water and the Na^+ content was determined by using a FP910 flame photometer (PG Instruments, Lutterworth, UK).

3.3 Human primary dermal fibroblasts (DF)

Human dermal fibroblasts were obtained from healthy individuals who had signed an informed consent. Collection of biospecimens for the isolation and culture of human dermal fibroblasts complied with the guidelines of the Helsinki Declaration and was approved by the local Ethics Committee of the University of Szeged, Hungary (CSR/039/00346-5/2015). Tissue samples were collected in accordance with the EU Member States' Directive 2004/23/EC on tissue isolation. Primary human DFs were isolated from a healthy individual who underwent plastic surgery [116]. Fibroblast cells were cultured in Dulbecco's modified Eagle's medium (DMEM; Gibco, Thermo Fisher Scientific, Waltham, Massachusetts, USA) supplemented with 10 % fetal bovine serum (FBS; Gibco, Thermo Fisher Scientific), 1% L-glutamine and 1% penicillin/streptomycin, incubated in a humidified incubator with 5 % CO_2 at 37 °C. Prior to *in vitro* experiments, the medium was replaced with DMEM without FBS for 24 hours. For real-time PCR measurements, DF cells were seeded in 96-well plates (Sarstedt, Nümbrecht, Germany) at a density of 10^4 cells/well (n=6 well/treatment group) and were exposed to culture medium with normal (Control; 150 mmol/L) or high sodium concentration (NaCl; 200 mmol/L) with or without recombinant human TGF-ß (1 nmol/L) (Thermo Fisher Scientific) at a total volume of 100ul.. Additional sodium concentration was determined as previously described [31]. Vehicle treated cells served as controls. After 24 hours, cells were harvested for real time PCR measurements.

3.4 Peripheral blood mononuclear cells (PBMCs)

Isolation and culture of human PBMCs has been approved by Semmelweis University Regional and Institutional Committee of Science and Research Ethics (31224-5/2017/EKU) after signing an informed consent. PBMCs from a healthy adult donor were isolated by density gradient centrifugation with at 800 x g for 20 minutes using Histopaque-1077 (Merck KGaA, Darmstadt, Germany). After isolation, the cells were plated into RPMI 1640 medium (ATCC, Manassas, Virginia, USA) supplemented with 10% FBS (Gibco, Thermo Fisher Scientific) and 1% penicillin/streptomycin solution

in 95% humidified air and 5% CO_2 at 37 °C. Prior to *in vitro* experiments, the medium was replaced with RPMI 1640 medium without FBS for 24 hours. For real time PCRs, PBMCs were seeded in 24 well plates (Sarstedt) at a density of 5×10^5 cells/well (n = 5 well/treatment group) and were exposed to culture medium with normal (Control; 150 mmol/L) or high sodium concentration (NaCl; 200 mmol/L) at a total volume of 500ul.

3.5 RNA isolation and cDNA synthesis

Total RNA was isolated from frozen skin samples, PBMCs and DFs using Total RNA Mini Kit (Geneaid Biotech Ltd., New Taipei City, Taiwan) according to manufacturer's instructions. Concentration and quality of isolated RNA were determined by DeNovix DS-11 spectrophotometer (DeNovix Inc., Wilmington, Delaware, USA). 2,500 ng of total RNA from skin and 50 ng of total RNA from PBMCs and DFs were reverse transcribed to generate first-stranded cDNA using Maxima First Strand cDNA Synthesis Kit for real time PCR (Thermo Fisher Scientific).

3.6 Real-time polymerase chain reaction (PCR)

Real-time PCRs were performed in a final volume of 20 µl containing 0.5 µM of forward and reverse primers (Integrated DNA Technologies, Coralville, Iowa, USA), 10 µl Light Cycler 480 SYBR Green I Master enzyme mix (Roche Diagnostics, Mannheim, Germany) and 1 µl cDNA in a LightCycler 480 system (Roche Diagnostics). The nucleotide sequences of the applied primer pairs were designed as previously described [117]. Their specific optimal annealing temperatures and product lengths are summarized in Table 1. The results were analyzed by Light-Cycler 480 software version 1.5.0.39 (Roche Diagnostics). The mRNA expressions were determined in comparison to the expression of *GAPDH* or *RPLP0* as a housekeeping gene from the same samples. Data were normalized and presented as the ratio of the mean values of their control groups.

Table 1. Nucleotide sequences of primer pairs, product length and specific annealing temperatures (Ta) applied for the real-time reverse transcriptase polymerase chain reaction (RT- PCR) detection.

Gene	Primer pairs		Product lenght	T_a
mouse ACTA2	F:	5'- CCC CTG AAG AGC ATC GGA CA -3'	105 bp	60 °C
	R:	5'- TGG CGG GGA CAT TGA AGG T -3'		
mouse COL1A1	F:	5'- CAA AGG TGC TGA TGG TTC T -3'	107 bp	60 °C

	R:	5’- GAC CAG CTT CAC CCT TG -3’		
mouse FN	F:	5'- GGT CAG GGC CGG GGC AGA T -3'	228 bp	60 °C
	R:	5'- CTG GCT GGG GGT CTC CGT GAT AAT -3'		
mouse GAPDH	F:	5'- ATC TGA CGT GCC GCC TGG AGA AAC -3'	164 bp	60 °C
	R:	5'- CCC GGC ATC GAA GGT GGA AGA GT -3'		
mouse ILβ	F:	5'- GCC ACC TTT TGA CAG TGA TGA GAA -3'	136 bp	55 °C
	R:	5'- GAT GTG CTG CTG CGA GAT TTG A -3'		
mouse IL10	F:	5'- CAA AGG ACC AGC TGG ACA ACA TAC -3'	124 bp	55 °C
	R:	5'- GCC TGG GGC ATC ACT TCT ACC -3'		
mouse IL13	F:	5'- ACG GCA GCA TGG TAT GGA GTG TGG -3'	161 bp	55 °C
	R:	5'- GGG GAG GCT GGA GAC CGT AGT GG -3'		
mouse IL17	F:	5'- AGG ACT TCC TCC AGA ATG T -3'	136 bp	60 °C
	R:	5'- TCA GGG TCT TCA TTG CGG -3'		
mouse MMP2	F:	5'-ACC ACC GAG GAC TAT GAC-3'	121 bp	60 °C
	R:	5'- TGT TGC CCA GGA AAG TGA -3'		
mouse MMP9	F:	5'- TGC CCT AGT GAG AGA CTC TAC A -3'	128 bp	60 °C
	R:	5'- CAG CGG TAA CCA TCC GA -3'		
mouse NLRP3	F:	5'- CTC TCC CGC ATC TCC ATT TGT AA -3'	141 bp	55 °C
	R:	5'- CTG CGT GTA GCG ACT GTT GAG G -3'		
mouse PDGFB	F:	5'- CTG GGC GCT CTT CCT TCC TCT C -3'	170 bp	60 °C
	R:	5'- CCA GCT CAG CCC CAT CTT CAT C -3'		
mouse TGFβ	F:	5'- GTG CGG CAG CTG TAC ATT GAC TTT -3'	239 bp	60 °C
	R:	5'- GGC TTG CGA CCC ACG TAG TAG AC -3'		
mouse TNFα	F:	5'- GGG CCA CCA CGC TCT TCT GTC TA -3'	83 bp	56 °C
	R:	5'- GCG CGG GAG GCC ATT TGG GAA CTT -3'		
human ACTB [117]	F:	5'- ACC GAG CGT GGC TAC AGC TTC ACC -3'	114 bp	53 °C
	R:	5'- AGC ACC CGT GGC CAT CTC TTT CTC G-3'		
human COL1A1	F:	5'- CTG CCC CGG CGC CGA AGT C -3'	96 bp	60 °C
	R:	5'- CCC TCG ACG CCG GTG GTT TCT TG -3'		
human FN	F:	5'- GGC TGC CCA CGA GGA AAT CTG C -3'	229 bp	58 °C
	R:	5'- GTG CCC CTC TTC ATG ACG CTT GTG -3'		
human GAPDH	F:	5'- AGC AAT GCC TCC TGC ACC ACC AA -3'	159 bp	60 °C
	R:	5'- GCG GCC ATC ACG CCA CAG TTT -3'		
human IL10	F:	5'- ATG CCC CAA GCT GAG AAC CAA GAC -3'	107 bp	60 °C
	R:	5'- AGA AAT CGA TGA CAG CGC CGT AGC -3'		
human IL13	F:	5'- CTG CAA ATA ATG ATG CTT TCG A -3'	90 bp	54 °C
	R:	5'- CCA GTT TGT AAA GGA CCT GCT CT -3'		
human VCL	F:	5'- CCA CGG CGC CTC CTG ATG C -3'	152 bp	60 °C
	R:	5'- GGC CTG AAT GCC TTC CAC TGT TGA -3'		
human VIM	F:	5'- GAG GCT GCC AAC CGG AAC AAT GAC -3'	203 bp	59 °C
	R:	5'- TCC TGC AGG CGG CCA ATA GTG TCT -3'		

3.7 LDH cytotoxicity assay

To perform LDH assay, DF cells were seeded (n=6 well/treatment group) into 96-well tissue culture plates at a density of $4x10^3$ cells/well. After 24 hours of incubation, cells were treated with culture medium containing increasing sodium concentration (150, 175, 200, 250 mM NaCl) for 24 hours. The extent of cell death was determined by a colorimetric method based on the activity of lactate dehydrogenase (LDH) enzyme in the supernatant, released from damaged cells. LDH assay was performed as previously described [118]. All reagents were purchased from Merck. Absorbance was recorded at 570 nm and at 690 nm as background in a SPECTROstar Nano microplate reader using SPECTROstar Nano MARS v3.32 software (BMG Labtech).

3.8 MTT cell proliferation assay

To perform MTT assay, DF cells were seeded (n=6 well/treatment group) into 96-well tissue culture plates at a density of $4x10^3$ cells/well. After 24 hours of incubation, cells were treated with culture medium containing increasing sodium concentration (150, 175, 200, 250 mM NaCl) for 24 hours. The rate of cell proliferation was determined by a colorimetric method based on the intracellular mitochondrial dehydrogenase activity of the adherent cells [119]. MTT cell proliferation and viability assay was performed by using Cell Proliferation Kit I (Roche Diagnostics) according to the manufacturer's recommendations. Absorbance was recorded at 570 nm and at 690 nm as background in a SPECTROstar Nano microplate reader using SPECTROstar Nano MARS v3.32 software.

3.9 Protein isolation and Western blot analysis

Dermal tissue samples from mice were homogenized in a lysis solution containing 50 mM HEPES, 150 mM NaCl, 1% Triton X-100, 5 mM EDTA, 5 mM EGTA, 20 mM sodium pyrophosphate, 20 mM NaF, 0.2 mg/mL phenylmethylsulfonyl fluoride, 0.01 mg/mL leupeptin, and 0.01 mg/mL aprotinin (pH 7.4) (each substance obtained from Merck). Protein concentration was determined by a detergent-compatible protein assay (BioRad, Hercules, CA, USA). Denatured samples (20 μg protein/lane) were loaded and separated on 4–20% gradient SDS polyacrylamide gel (BioRad), thereafter transferred to nitrocellulose membranes (BioRad). Pre-stained protein standard (BioRad) was used as molecular weight marker. To verify the transfer, membranes were stained with Ponceau

S (Sigma-Aldrich), then washed and blocked with 5% non-fat milk in TRIS-buffered saline (TBS) for 1 hour at room temperature. They were then incubated overnight at 4 °C with antibodies specific for phosphorylated (p)-SMAD2/3 (sc-11769; 1:500, Santa-Cruz Biotechnology) or GAPDH (sc-47724; 1:2000, Santa Cruz Biotechnology). After repeated washing with TBS containing 0.05% Tween-20 and 1% non-fat milk, membranes were incubated with the adequate horseradish peroxidase (HRP)- conjugated secondary antibodies (1:1000 anti-rabbit or 1:5000 anti-mouse, Santa Cruz Biotechnology) for 1 hour at RT. Immunoreactive bands were developed by enhanced chemiluminescence detection (Immobilon Forte Western HRP substrate, Merck KGaA) and the resulted images were visualized with VersaDoc 5000MP system (Bio-Rad) and analyzed with Quantity One v4.6.9 (Bio-Rad) and ImageJ 1.48v (National Institutes of Health, Bethesda, MD, USA) softwares. Relative protein levels were determined in comparison to GAPDH as protein loading control. Data were normalized and presented as the ratio of the mean values of the control group.

3.10 SiriusRed collagen detection assay

For the SiriusRed assay, human DF cells were seeded in 96-well plates (Sarstedt) at a density of 10^4 cells/well (n = 5 well/ treatment group) and were exposed to culture medium with normal (Control; 150 mmol/L) or high sodium concentration (NaCl; 200 mmol/L) with or without recombinant human TGF-ß (1 nmol/L) (Thermo Fisher Scientific) for 24 hours at 37 °C. Collagen deposition was determined based on a histological dye SiriusRed, incorporating into the triple helical collagen molecules. The assay was performed as previously described [120]. All reagents were purchased from Merck. Absorbance was determined at 544 nm and at 690 nm as background in a SPECTROstar Nano microplate reader using SPECTROstar Nano MARS v3.32 software.

3.11 Immunocytochemistry and cell morphology analysis

Human DF cells were seeded in cell culture chambers (Sarstedt) at a density of 10^4 cells/well and were exposed to culture medium with normal (Control; 150 mmol/L) or high sodium concentration (NaCl; 200 mmol/L) for 24 hours at 37 °C. After washing with WashPerm solution, slides were permeabilized with Cytofix/Cytoperm (BD Pharmingen, San Diego, California, USA) for 15 minutes at room temperature. Slides were incubated with primary antibody specific for α-SMA (mouse, 1:1000; MERCK,

Darmstadt, Germany) for 1 hour at room temperature. The slides were then washed and incubated with suitable Alexa Fluor 488 conjugated secondary antibody (anti-mouse, 1:100; Invitrogen, Thermo Fisher Scientific) in the dark for 30 minutes at room temperature. Thereafter, slides were covered with ProLong Gold antifade reagent (Invitrogen, Thermo Fisher Scientific). Correspondent controls were performed by omitting the primary antibodies to ensure their specificity and to avoid autofluorescence. Circularity evaluation of α-SMA immunopositive DFs was performed by graphical analysis using ImageJ 1.48v software. Images of 35–40 randomly selected cells from each treatment group were taken with Olympus IX81 fluorescent microscope (Olympus, Japan). The circularity of the fibroblasts was calculated according to the following formula: circularity=4*π(area/perimeter^2). If the circularity of a cell is 1, then the shape of the cell is round, and as the shape deviates from the circle, the value decreases.

3.12 *In vitro* scratch assay

To perform scratch assay, MRC-5 cells were seeded (n=6 well/treatment group) in 12-well tissue culture plates (Sarstedt) at a density of $4x10^5$ cells/well. After 24 hours of incubation, media was aspired from cells and the monolayer was scratched with a single firm movement using a 200 µl pipette tip. The wells were washed three times with 2 ml of sterile PBS to remove debris and non-adherent cells, thereafter cells were treated with recombinant EGF diluted in 1 ml culture medium containing 0.1% FBS.

3.13 Transient agarose spot (TAS) migration assay

To perform TAS assay, 2 µl of hot 0.1% agarose (Merck) solution (diluted in distilled H_2O) was pipetted in the center of each well of a 96-well tissue culture plate (Sarstedt), then the gel droplets were allowed to polymerise at room temperature for 15 minutes. Thereafter, MRC-5 cells and human dermal fibroblasts were seeded (n=6-8 well/treatment group) at a density of $2x10^4$ cells/well to reach near full confluence. After 24 hours of incubation, media was aspired from cells and the agarose barriers were carefully removed with a 100 µl pipette. The wells were washed three times with 200 µl of sterile PBS to remove debris and non-adherent cells. Thereafter MRC-5 cells were treated with recombinant EGF diluted in 1 ml culture medium containing 0.1% FBS, while DFs were treated with culture medium containing normal (Control; 150 mM) or high sodium concentration (NaCl; 200 mM). Brightfield images of each well were taken

using Olympus IX81 microscope system (Olympus) at 0, 24 and 48 hours after treatment. Cell-free gap area was measured using ImageJ 1.48v software (National Institutes of Health) and determined as a ratio (%) of initial gap area at 0 hour:

$$\text{gap area } [\%] = \frac{\text{actual gap area}}{\text{initial gap area}} \times 100$$

3.14 Statistical analysis

Statistical evaluation of data was performed by GraphPad Prism 7.0 Software (GraphPad Software, La Jolla, California, USA). To test if the the groups show a normal distribution, Kolmogorov-Smirnov normality test was performed. In the case of a normal distribution, the data were analyzed by an unpaired t-test, otherwise a Mann-Whitney U-test was performed. Multiple comparisons of the raw data derived from migration assays were performed by using multiple t-test and ordinary two-way ANOVA with Dunnett correction. Pearson's correlation was used for correlation analyses. Data were normalized and presented as the ratio of the mean values of their control groups. $p \leq 0.05$ was considered as statistically significant. Unless otherwise indicated, results are illustrated as mean+SD of the corresponding treatment groups. The applied tests, significances, number of elements (n) are indicated in each figure legend.

4. Results

4.1 Effect of high salt loading on dermal inflammation and tissue remodeling *in vivo* and *in vitro*

4.1.1 Effect of 8% NaCl diet on body weight

In our preliminary experiments we investigated whether the high salt diet (HSD) containing 8% NaCl has an effect on the body weight of mice. Our results showed that there was no significant difference in body weight between animals on NSD and those on HSD even after two weeks, which is consistent with the results of other research groups (Fig 5) [121-123].

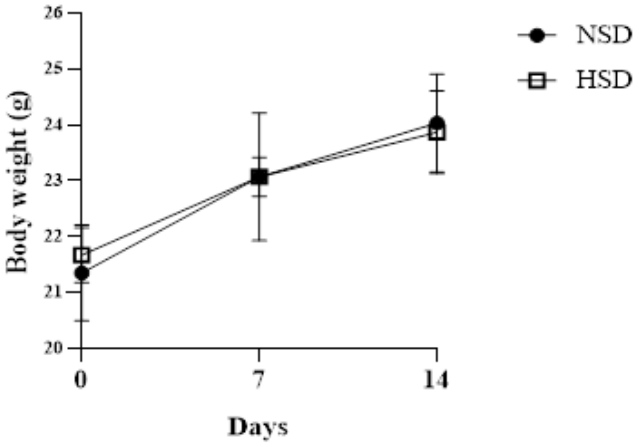

Figure 5. Effect of high salt diet on body weight.
Mice were kept on NSD or HSD for 14 days. The body weight was measured in every 7 days. (n=6 in each group).

4.1.2 Effect of imiquimod (IMQ) on dermal inflammation

To investigate the effect of high salt diet on dermal inflammation, IMQ was administered topically for 5 days to the backs of mice after 4 weeks of receiving NSD or HSD detailed in Figure 6/a (Fig 6/a). IMQ application induced remarkable dermatitis-like symptoms such as red, thickened and dry skin (Fig 6/b).

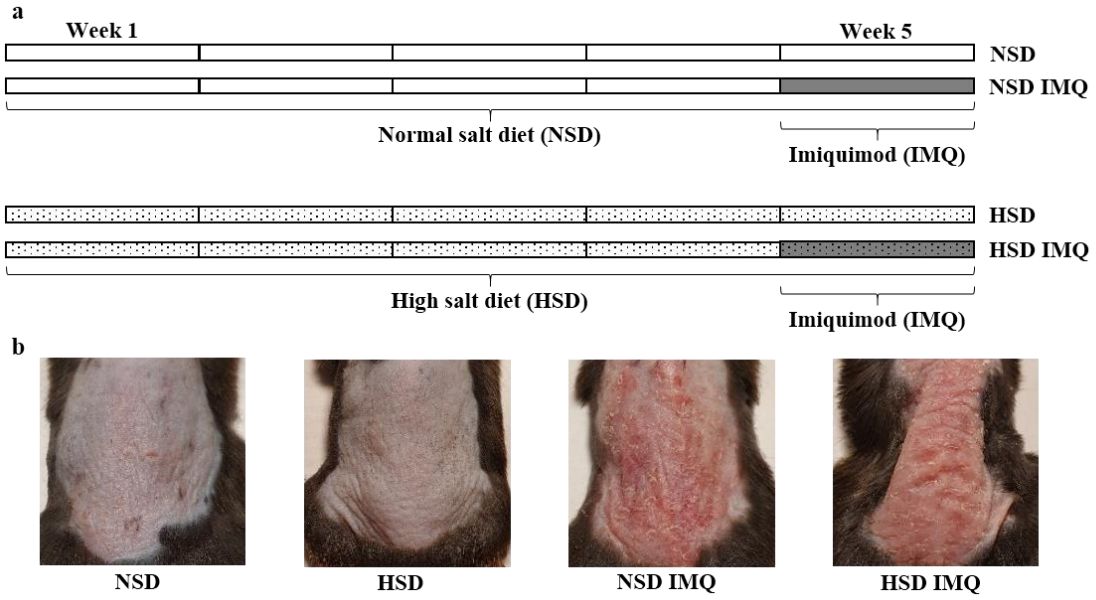

Figure 6. Effect of imiquimod on dermal inflammation

(**a**) Mice were kept on NSD or HSD for 5 weeks and on the last 5 days of the dietary regime the mouse model of IMQ-induced dermatitis was performed on the indicated group of animals. (**b**) 5 days of IMQ (62.5mg with 5% imiquimod cream) treatment applied to NSD and HSD mice resulted in the inflammation of the dorsal skin of mice compared to vaseline treatment.

4.1.3 Effect of high salt diet on dermal inflammatory cytokine expression

We examined whether high salt intake affects the inflammatory cytokine and Na^+ content of the skin in the experimental model described previously (Fig 6/a). According to our data, HSD increased the sodium content of the skin (Fig 7/a). IMQ increased the dermal mRNA expression of *Il1b, Il17, Tnfa, Il10 and Nlrp3* (Fig 7/b-f) in NSD group. Dermal mRNA expression of *Il17* was increased in HSD group compared to NSD (Fig 7/c). The mRNA expression of *Il10* was lower in the skin of HSD IMQ group compared to that of NSD IMQ group (Fig 7/f). Furthermore, mRNA expression of *Il13* was decreased in both HSD and HSD IMQ group compared to that of NSD and NSD IMQ group (Fig 7/g).

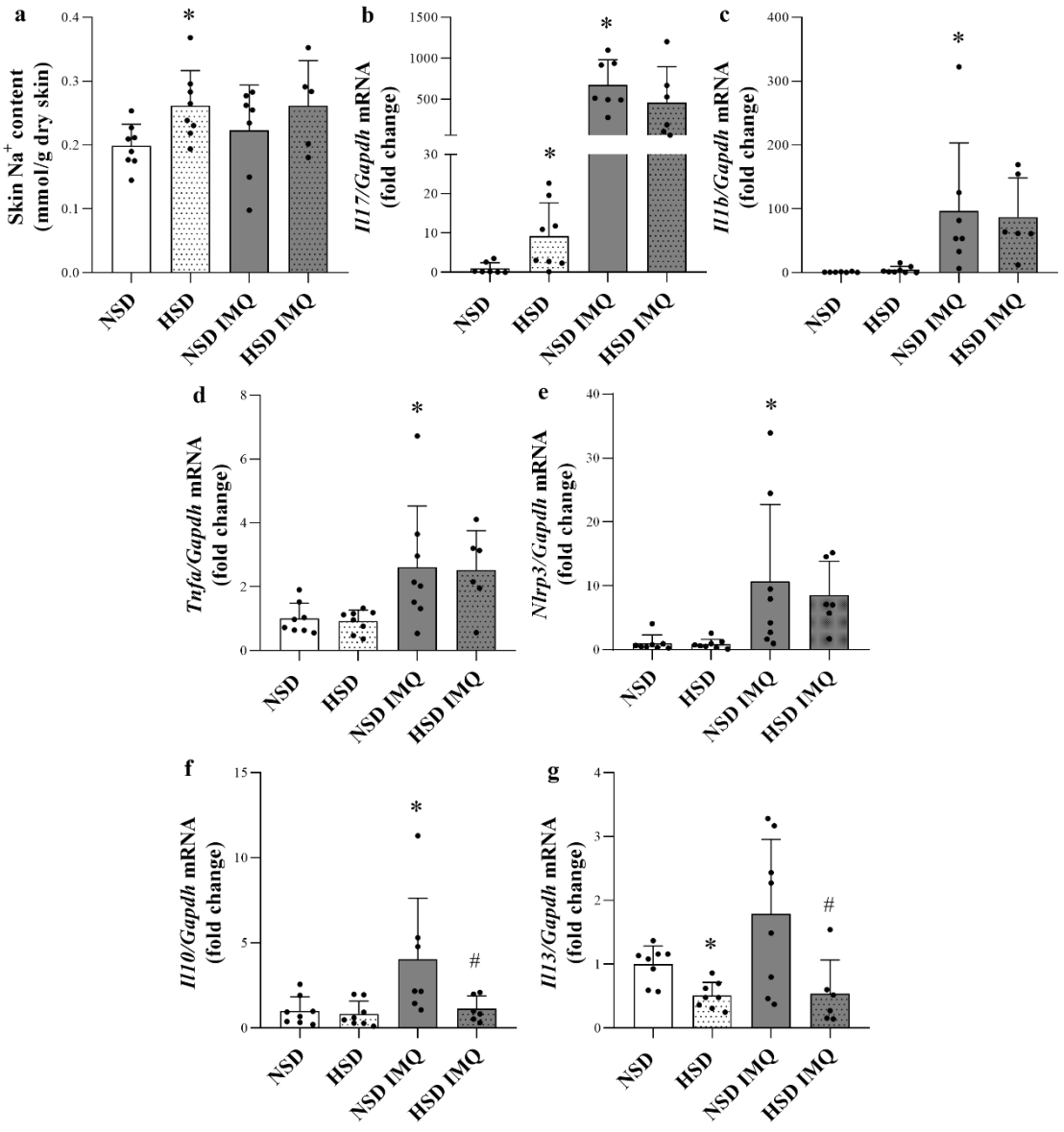

Figure 7. Effect of high salt diet on dermal inflammation in IMQ-treated and control mice.

(**a**) The skin Na^+ content was measured by flame photometry following tissue digestion. (**b-h**) The dermal mRNA expression of *Il17*, *Il11b*, *Tnfa*, *Nlrp3, Il10,* and *Il13,* in the skin tissues of mice were determined by real-time PCR. Values were expressed as mean+SD normalized to the *Gapdh* housekeeping gene, dots represent individual values. n=6-8 in each group; *p<0.05 vs. NSD; #p<0.05 vs. NSD IMQ; (Unpaired t-test (a,d,f,g), Mann-Whitney U-test (b,c,e,h)).

4.1.4 Effect of high salt environment on the anti-inflammatory and profibrotic cytokine production of human PBMCs

To investigate whether the high salt loading is responsible for the decreased production of immune cell- derived anti-inflammatory *IL10, IL13* and profibrotic *PDGF-B* in the skin, we investigated its effect on PBMCs. Cells were treated with 200 mM NaCl medium, as this concentration is often used in the literature and is the highest concentration that did not affect either cytotoxicity or proliferation according to our measurements (Fig 9/a,b). According to our results high NaCl loading inhibited the mRNA expression of *IL10, IL13* and *PDGF-B* of human PBMCs (Fig 8/a,b,c).

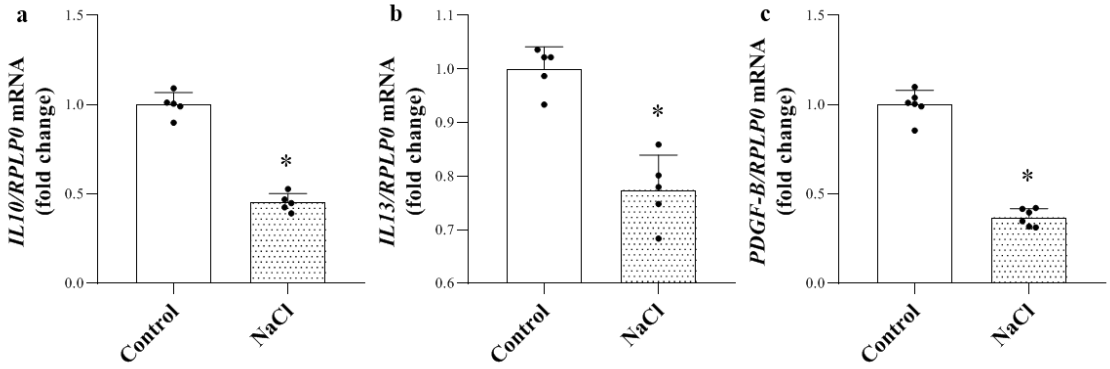

Figure 8. Effect of high NaCl environment on the anti-inflammatory and profibrotic cytokine production of human PBMCs

(**a-c**) The mRNA expression of *IL10*, *IL13* and *PDGF-B* were measured by real-time PCR. Values were expressed as mean+SD normalized to the *RPLP0* housekeeping gene, dots represent individual values. n=5 in each group; *p<0.05 vs. Control (Unpaired t-test).

4.1.5 Effect of high NaCl condition on cell death and cell proliferation of DFs

To investigate the effect of high salt environment on the viability and proliferation of DFs we used various concentrations of additional NaCl in the cell culture media. To investigate the effect of NaCl concentration of the medium used in our *in vitro* experiments, we examined the effect of each concentration on the viability and proliferation of DFs (Fig 9/a,b).

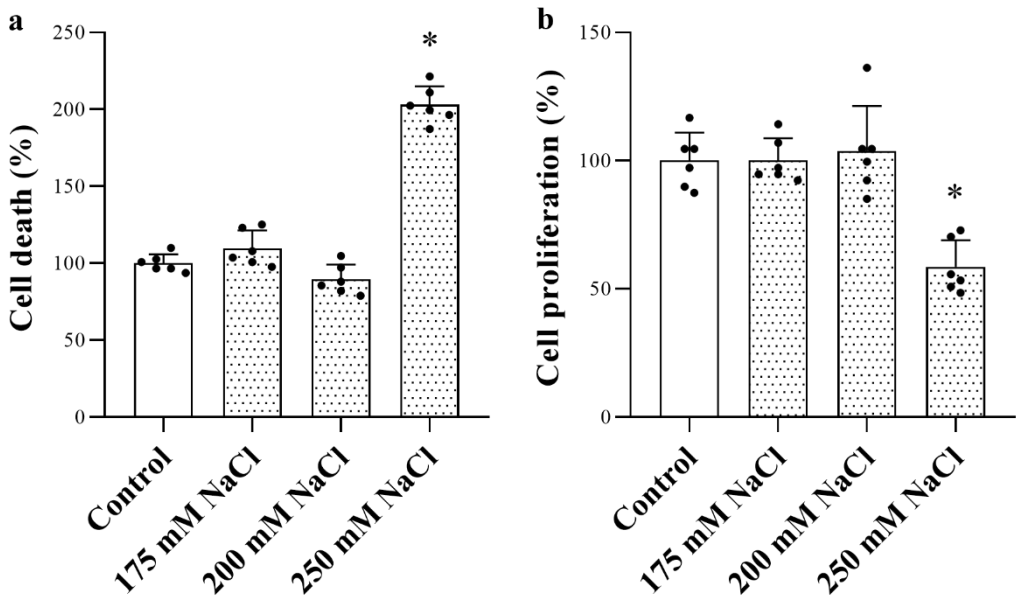

Figure 9. Effect of high NaCl condition on cytotoxicity and cell viability of DFs
(**a**) To monitor cytotoxicity, LDH assay was performed on cell supernatants. (**b**) The proliferation of DFs was investigated by MTT assay. n=5 in each group; *p<0.05 vs. Control (Unpaired t-test).

4.1.6 Effect of high salt diet on dermal ECM remodeling and skin thickness

To investigate the effect of excessive dietary salt intake on tissue remodeling ECM markers, dermal thickness and the levels of profibrotic phosphorylated (p)SMAD2/3 protein were studied in the above experimental setting (Fig 6/a). We found that dermal mRNA expression of *Acta2*, *Col1a1* and *Fn* was decreased in HSD IMQ group compared to that of NSD IMQ group (Fig 10/a-c). In addition to the ECM markers, ECM remodeling-related growth factors and enzymes in vehicle and IMQ-treated mice were also investigated. We found that dermal mRNA expression of *Pdgfb* was decreased in HSD and HSD IMQ groups compared to that of NSD and NSD IMQ groups. (Fig 10/d). *Tgfb* was not affected by salt diet, but the IMQ treatment increased its amount in the skin (Fig 10/e). Skinfold thickness on the backs of the mice in the IMQ group was significantly increased by IMQ treatment compared with subjects from the control group, nevertheless the skin of the mice who were kept on HSD was thinner than the control group among the IMQ treated mice (Fig 10/f). Moreover, the protein amount of pSMAD2/3 was significantly decreased in HSD IMQ group compared to NSD IMQ group (Fig 10/g).

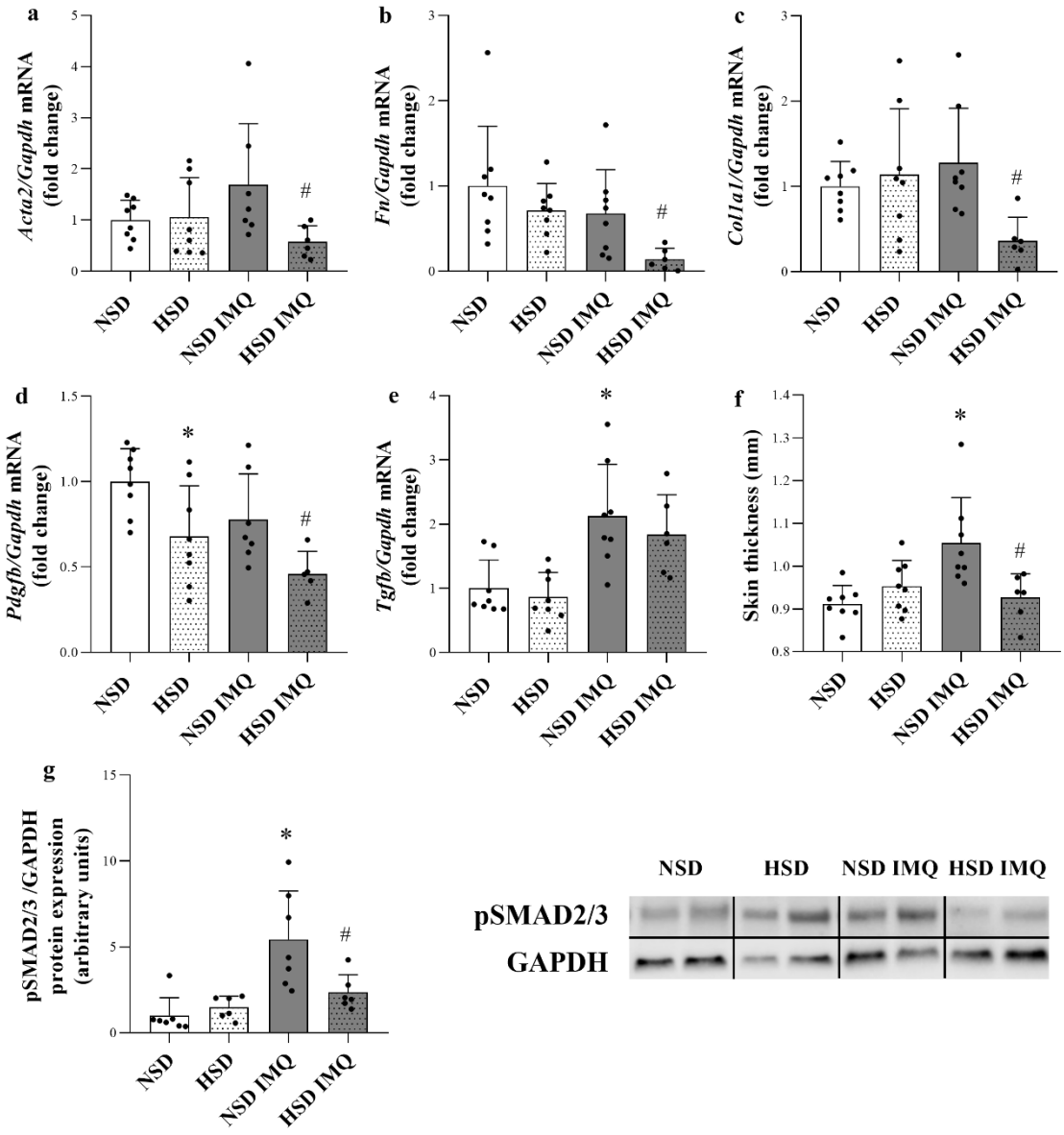

Figure 10. Effect of high salt diet on ECM marker production and dermal tissue remodeling-associated factors of IMQ-treated and control mice.

(**a-e**) The dermal mRNA expression of *Acta2, Fn, Col1a1*, *Pdgfb*, *Tgfb* and *Ctgf* in the skin tissues of mice was determined by real-time PCR in comparison with *Gapdh* as internal control. (**f**) The skinfold thickness on the backs of the mice was measured with a caliper at the termination of the experimental model. (**g**) The dermal protein expression of (p)SMAD2/3 in the skin tissues of mice was determined by Western blot in comparison with GAPDH as protein loading control. Protein samples from control and IMQ-treated mice were run on separate gels. They were compared based on internal control. Values were expressed as mean+SD, dots represent individual values. *n*=6-8 in each group;

*p<0.05 vs. NSD; #p<0.05 vs. NSD IMQ; (Unpaired t-test (a,b,d,f), Mann-Whitney U-test (c,e,g)).

4.1.7 Effect of high NaCl concentration on dermal ECM degradating enzymes

To investigate the effect of high dietary salt diet on dermal tissue remodeling, we also examined the expression of enzymes mediating ECM turnover. We found that dermal mRNA expression of *Mmp2* and *Mmp9* was increased by salt intake in control animals (Fig 11/a-b).

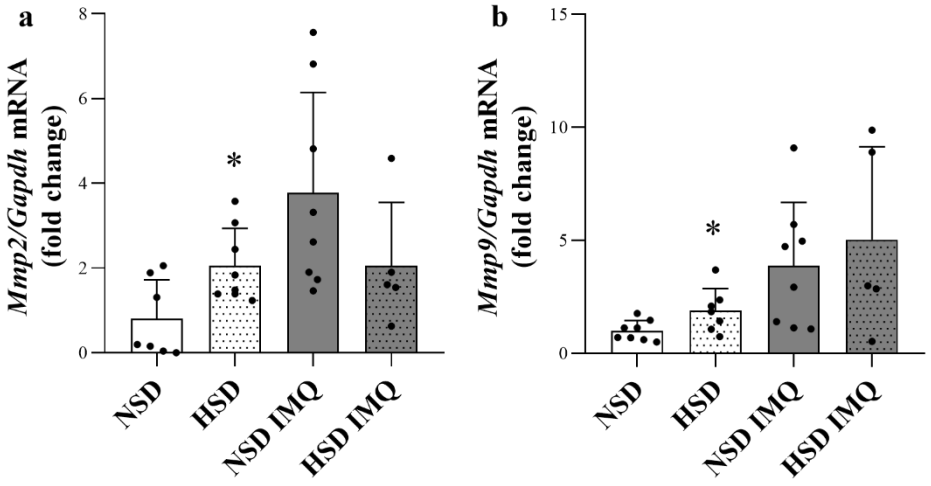

Figure 11. Effect of high NaCl concentration on enzymes responsible for the degradation of the ECM of IMQ-treated and control mice

(**a-b**) The dermal mRNA expression of *Mmp2* and *Mmp9* in the skin tissues of mice was determined by real-time PCR in comparison with *Gapdh* as internal control. Values were expressed as mean+SD, dots represent individual values. *n*=6-8 in each group; *p<0.05 vs. NSD; (Unpaired t-test (a), Mann-Whitney U-test (b)).

4.1.8 Effect of high NaCl environment on the cell motility of human primary dermal fibroblasts

The effect of increased NaCl concentration on cellular morphology was visualized by α-SMA immunofluorescence staining on the cytoskeleton of human DFs *in vitro*. While control cells had elongated shape, flattened and more circular morphology was observed for high salt loaded cells. Accordingly, quantitative determination of the shape of dermal fibroblast cells showed significantly elevated circularity in the high salt treated

group (Fig 12/a). Furthermore, the mRNA expression of fibroblasts motility regulator *VIM*, *VCL* and *ACTB* decreased in the high salt treated group (Fig. 12/b-d). Consistent with these results, larger cell-free area indicating reduced migration capacity was observed in the high salt-treated DFs at both 24 and 48 hours of the experiment (Fig 12/e).

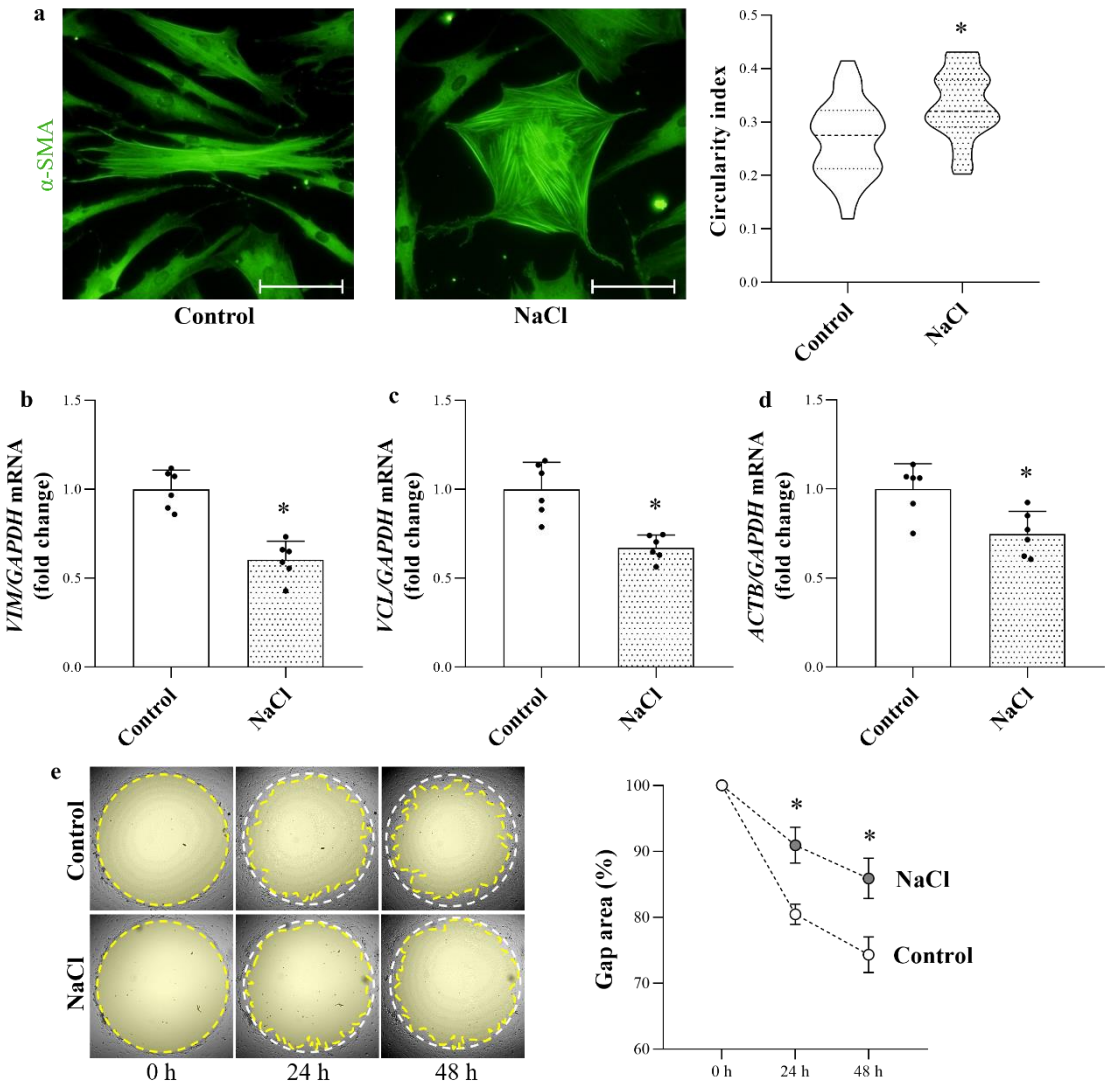

Figure 12. Effect of high NaCl concentration on human primary dermal fibroblast cells.

(**a**) Cellular morphology of the cells was visualized by α-SMA immunofluorescent staining (green). Scale bar: 20 μm (**a**) Determination of circularity of α-SMA immunopositive human primary dermal fibroblasts was carried out by graphical analysis of the cells (n=35-40). Values were expressed as mean+SD. $^{*}p<0.05$ vs. Control (Unpaired t-test). (**b-d**) The mRNA expression of cell motility markers *VIM*, *VCL* and *ACTB* in the human dermal fibroblasts was determined by real-time PCR (n=6). Values

were expressed as mean+SD normalized to the *GAPDH* housekeeping gene, dots represent individual values. *p<0.05 vs. Control; (Unpaired t-test (b,c), Mann-Whitney U-test (d)). (**e**) The migration of DFs was determined by TAS assay, measuring the size of the cell-free gap area at 0, 24 and 48 hours (n=8). Values were expressed as mean+SD, dots represent individual values. *p<0.05 vs. Control (two-way ANOVA + Sidak's multiple comparisons).

4.1.9 Effect of high NaCl environment on the ECM marker production of human primary dermal fibroblasts

Since DFs are the main sources of skin ECM, we examined the direct effect of salt loading on their functional activity. Consistent with our *in vivo* results in IMQ-treated animals, increased salt concentration in culture media reduced both endogenous and TGF-β-induced *FN* and *COL1A1* production in DFs (Fig 13/a-b). According to these findings, high NaCl environment decreased the collagen deposition of DFs, as well (Fig 13/c).

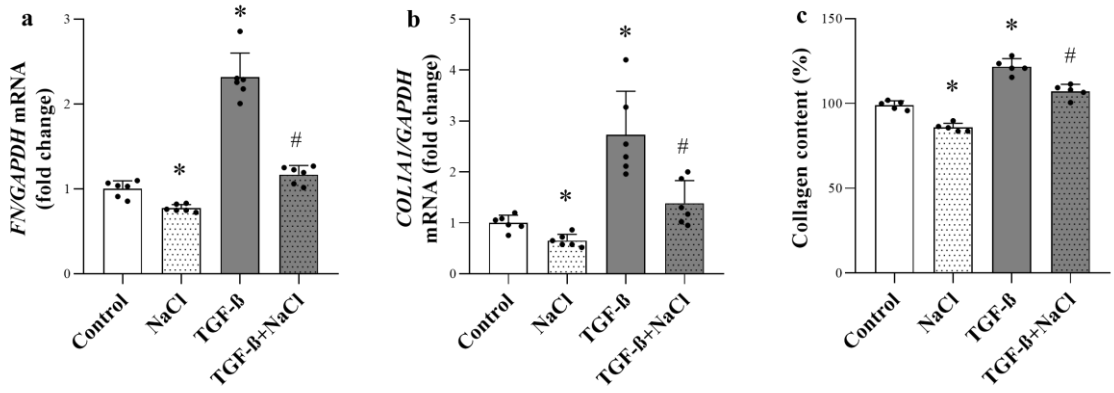

Figure 13. Effect of high NaCl concentration on the ECM marker production of human primary dermal fibroblasts.

(**a-b)** The mRNA expression of *FN* and *COL1A1* in the human dermal fibroblasts was determined by real-time PCR. (**c**) The proportion of collagen content in human DFs was detected by SiriusRed collagen detection assay. Values were expressed as mean+SD normalized to the *GAPDH* household gene, dots represent individual values. (n=6 in each group); *p<0.05 vs. Control; #p<0.05 vs. TGF-ß; (Unpaired t-test (b,c), Mann-Whitney U-test (a)).

4.2 Transient Agarose Spot (TAS) assay: a new method to investigate cell migration

4.2.1. Basic settings of TAS assay: agarose spot stability and optimal cell density

The stability of agarose gel spots was examined for several consecutive days using MRC-5 lung fibroblasts. Gel spots were removed 24 hours after cell seeding in 'transient' group, thereafter the rapid reduction of cell-free gap area was observed. In contrast, when the agarose gel spots were not removed ('permanent' group), the covered area remained cell-free for days, without any signs of cell migration under agarose, allowing to change the medium and initiate the examination of migration at any time after optional pre-treatment steps (Fig 14/a-b).

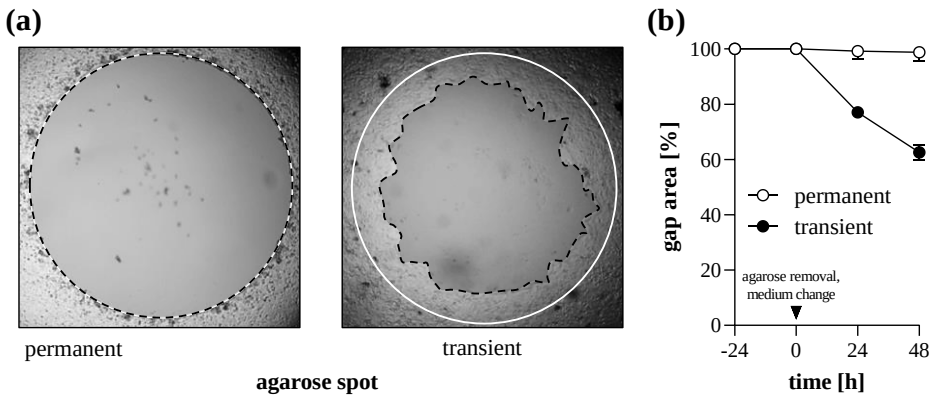

Figure 14. Gap closure in the case of permanent and transient agarose spots.
TAS migration assay was performed on MRC-5 cells to examine the stability of agarose gel spots. **(a)** After brightfield microscopic imaging, cell-free zone areas were analysed graphically. In the representative images, the lines indicate the area of the gap at 0 (white) and 48 (black) hours after gel removal. **(b)** Gap closure was monitored for 72 hours after cell seeding. Values were expressed as mean+SD (n=6 in each group).

4.2.2 TAS assay as fibroblast migration assay

Cell migration of MRC-5 lung fibroblasts was investigated by TAS assay following EGF treatment. We found that addition of EGF into the culture media increased the rate of gap closure (Fig 15/a-b).

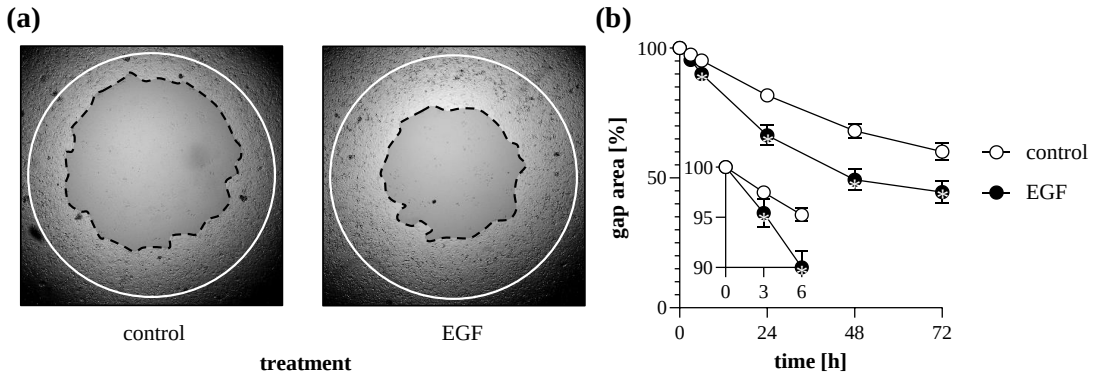

Figure 15. Effect of growth factor treatment on gap closure.

To determine the effect of EGF treatment, TAS migration assay was performed on MRC-5 cells. **(a)** Cell-free zone areas were analysed graphically after brightfield microscopy. Lines in representative images indicate the gap edges at 0 (white) and 48 (black) hours after gel removal. **(b)** The gap closure was monitored for 72 hours after gel removal. Values were expressed as mean+SD (n=8 in each group); *p<0.05 vs. 0% control at the concerning time (two-way ANOVA).

4.2.3 Comparison of scratch and TAS migration assays

Comparison of sensitivity and reproducibility of scratch and TAS migration assays was performed on MRC-5 cells. Based on several independent experiments, we confirmed that while the confidence interval of initial gap size varied between 23-30% in case of scratch assay, it was only around 9% in case of TAS assay (Fig 16/a). In addition to the inconsistent size, the gap closure of scratched area is uneven and can only be documented by a series of images. In contrast, the entire cell-free area can be examined in one single field of view in case of the TAS assay (Fig 16/b). The gap closure of MRC-5 cells showed similar kinetics in case of scratch (Fig 16/c) and TAS (Figure 15/d) migration assays. Nevertheless, the intra-group variance determined by the coefficient variation of group means was on average 3-fold higher in scratch assay compared to TAS assay, in case of relative (Fig 16/c-d) gap size values.

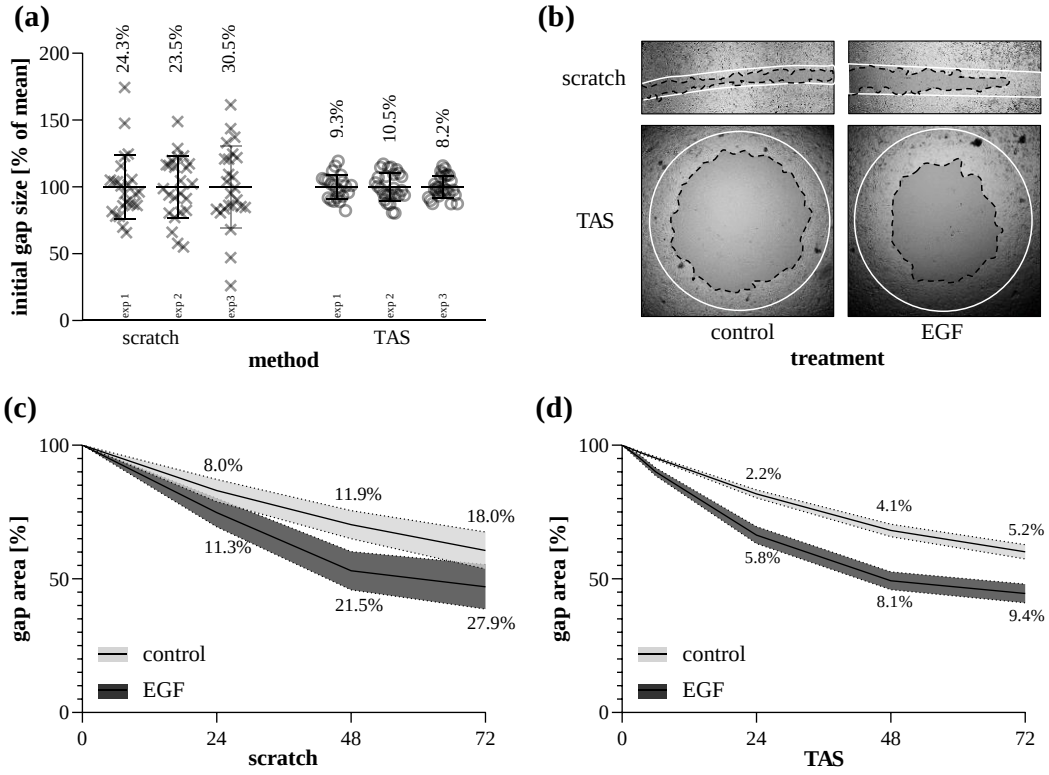

Figure 16. Reproducibility of scratch and TAS migration assays.

(a) Consistency of initial gap sizes was defined in independent experiments performed on MRC-5 cells (n=24-30 in each 3-3 experiments). Percentage values indicate the coefficient variation of the concerning groups. **(b)** Evenness of gap closure was examined on control and EGF-treated cells, as demonstrated by representative microscopic images. In the representative images, the lines indicate the gap edges at 0 (white) and 48 (black) hours after gel removal. Gap closure kinetics of control and EGF-activated MRC-5 cells were examined by **(c)** scratch and **(d)** TAS migration assays. **(c-d)** Alteration in gap size was determined by relative (percentage of initial size) values. Values were expressed as mean+SD, where line widths and percentage values indicate the coefficient variation of the concerning groups (n=6 in each group).

5. Discussion

5.1. Effect of high salt diet on dermal tissue remodeling

Nowadays, increasing salt intake is a global problem. The extensive pathological effects of high dietary salt consumption have been revealed in numerous studies. The dietary salt intake is the main source of Na^+ for our body. Although the skin is our largest Na^+ storage organ, its effect on skin homeostasis is not completely understood. Therefore, one of the main aims of my PhD work was to investigate the effect of high salt intake and the consequent elevated local Na^+ concentration on dermal pathological processes including inflammation and tissue remodeling.

The salt storage capacity of the skin has been described in the early 1900s, but comprehensive researches have only been carried out in recent years, which have begun to study the mechanisms by which salt is stored and what effects it may have. [124]. Titze et al. pioneered the study of tissue Na^+ storage resulting from increased salt intake, and its physiological effects, such as enhancing skin barrier function by increasing macrophage activation, maintaining volume homeostasis despite increased total body Na, increasing interstitial osmolality, or its interaction with GAGs [19, 21, 23, 125]. Numerous animal experimental studies have demonstrated that a significant proportion of excessive dietary sodium is stored in the skin in an osmotically active as well as GAG-bound inactive form [19-25, 46]. Our chemical analysis also confirmed accumulated dermal sodium content due to high salt intake in mice (Fig 7/a). In addition, high-resolution ^{23}Na-MRI imaging has made it possible to detect dermal sodium stores non-invasively in humans, demonstrating the epidermal and subepidermal accumulation of Na^+ [126]. The quantitative analysis showed that dermal salt storage increased with age [127]. Changes in skin structure with aging also include a decrease in the amount of GAG, which may lead to decreased dermal Na^+ content due to lower Na^+-binding capacity. Interestingly, higher Na^+ concentrations were measured in the skin of men than in women [126, 128]. It remains unclear whether these differences reflect variations in Na^+ metabolism or possibly the effect of other factors such as skin thickness and lipid content, which may differ between the sexes.

According to the literature, local sodium excess and high salt diet induce inflammatory cytokine production in cells of the innate and adaptive immune system, thereby exacerbating existing pathological processes in many organs, including the lungs,

kidneys, intestinal tract, and central nervous system [46, 50, 52, 129, 130]. It is also known that in some skin diseases, such as atopic dermatitis or acute cellulitis, the Na^+ content of the skin is elevated, however, the exact effect of increased local Na^+ concentration on the pathological processes of the skin has not been elucidated [19, 37]. Therefore, we investigated the effect of a high salt diet and the resulting local Na^+ excess on inflammation and related tissue remodeling using an IMQ-induced dermatitis model.

The IMQ application induced remarkable dermatitis, as expected (Fig 6/b). It increased the dermal mRNA expression of various cytokines *Il1b, Il10, Il17, Tnfa*, and *Nlrp3* (Fig 7/b-f). The expression of *Il10* and *Il13* was altered by high salt diet in the IMQ treated mice (Fig 7/f,g)

Our results demonstrated for the first time, that high salt diet increased the proinflammatory IL-17 cytokine expression in the skin of mice (Fig 7/b). These results are consistent with literature data demonstrating that increased local Na^+ concentrations promote the expression of IL-17 cytokine produced by Th17 cells [38, 59].

IL-10, produced by lymphocytes and monocytes, is generally considered to be the quintessential anti-inflammatory cytokine via its inhibitory effect on pro-inflammatory cytokine release and antigen presentation of various immune cells [131, 132]. Its ability to reduce inflammation and promote wound healing is well documented [133].

Similarly, IL-13 is also an anti-inflammatory cytokine that inhibits the M1 macrophages expressing proinflammatory mediators, while promotes the activation of anti-inflammatory M2 macrophages [134, 135]. Therefore, our results suggest that HSD associated decreased dermal cytokine expression of anti-inflammatory IL-10 and IL-13 may exacerbate IMQ-induced dermatitis.

Since the main sources of the aforementioned IL-10 and IL-13 cytokines are the immune cells, including lymphocytes and monocytes, we examined whether salt loading affects the production of *IL10* and *IL13* of peripheral immune cells [136-138]. Consistent with our *in vivo* results, the high salt environment reduced the expression of both *IL10* and *IL13* in PBMCs (Fig 8/a,b). The direct effect of salt loading on immune cells may explain the decreased anti-inflammatory cytokine expression in the skin of animals on high salt diet. In addition, the anti-inflammatory IL-10 signaling directly suppresses Th17 cells, and IL-13 also negatively regulates IL-17 expression through an IL-10-dependent mechanism. These results suggest that the changes in the expression of pro- and anti-

inflammatory cytokines associated with high salt diet may enhance the inflammatory processes in the skin.

Inflammation is a major regulator of ECM remodeling by inducing the effector cells, growth factors, and enzymes responsible for the production and degradation of ECM components [139]. The DF-mediated ECM remodeling plays a crucial role in dermal wound healing [140]. Therefore, we examined whether the increased Na^+ content and decreased presence of anti-inflammatory cytokines in the skin of mice on high salt diet affect the major cellular and structural elements of ECM. Our results showed that the expression of α-SMA *(Acta2)*, a specific marker of active DFs decreased in the skin of IMQ-treated mice on HSD compared to NSD IMQ mice (Fig 10/a). Based on literature data, dermal α-SMA expression is proportional to the activity and number of DFs, which are responsible for the production of ECM architecture components, including collagens and fibronectin [140-142]. Accordingly, in our *in vivo* experiment, dermal mRNA expression of both *Col1a1* and *Fn* was decreased in the HSD IMQ group compared to the NSD IMQ group (Fig 10/b,c). Taken together, our results suggest that in the presence of an inflammatory condition, high salt intake inhibits the ECM production of DFs. Interestingly, despite the fact that inflammation induces the production of ECM components in most organs, increased salt intake reduced ECM synthesis in the dermatitis model.

Investigating the underlying molecular mechanisms of high salt diet mediated ECM alterations, we focused on the expression of mitogenic growth factors responsible for the proliferation and ECM production of DFs. PDGF-B is considered as the main profibrotic growth factor, inducing the proliferation and ECM synthesis of fibroblasts in various organs, including the skin. Our results demonstrated that dermal expression of PDGF-B was decreased in both the HSD and HSD IMQ groups compared to controls (Fig 10/d). Therefore, our results suggest that diminished expression of α-SMA and ECM components in HSD IMQ mice is closely related to the decreased amount of the PDGF-B [143, 144]. Immune cells play a crucial role in the production of profibrotic growth factors, therefore, we examined the effect of high salt loading on their PDGF-B production [145, 146]. We found that the high salt environment reduced the *PDGFB* production of PBMCs, suggesting a possible mechanism underlying the decreased dermal *Pdgfb* expression in mice on HSD.

Our data demonstrated that IMQ treatment resulted in increased mRNA expression of profibrotic *Tgfb*, however its expression was not altered by high salt diet. TGF-ß is another growth factor regulating tissue remodeling and has been considered as a main activator of fibroblast proliferation and ECM synthesis. An interesting contradiction is that while HSD did not reduce IMQ induced *Tgfb* expression, the amount of *Acta2*, *Col1a1*, and *Fn* was significantly decreased in the skin of IMQ-treated mice due to elevated salt intake (Fig 10/a-c, e). Since the TGF-ß induced Smad transcription factors mediated signaling pathway plays a pivotal role in the development of tissue remodeling in almost all organs, we examined the effect of salt intake on the expression of Smad2/3, which is a central element of the TGF-β/Smad signaling pathway [95, 147, 148]. Our results showed that the level of activated, phosphorylated (p)-Smad2/3 protein was reduced in the skin of HSD IMQ mice compared to the NSD IMQ group (Fig 10/g). Several studies have previously demonstrated that decreased Smad2/3 synthesis or pharmacological inhibition of TGF-β/Smad signaling reduces the expression of ECM remodeling markers [95]. Therefore, the decreased dermal pSmad2/3 level may also explain the decreased expression of ECM components in the skin of HSD IMQ mice. Besides TGF-ß, IL-13 cytokine has also been shown to facilitate Smad2/3 phosphorylation in primary human dermal fibroblasts [149-152]. In addition to the above, the role of IL-13 in dermal tissue remodeling has been demonstrated in numerous studies. Indeed, during cutaneous wound healing, IL-13 promotes the chemotaxis and proliferation of DFs, and induces the production of ECM components, while disproportionately increased activity of IL-13 leads to abnormal collagen homeostasis, contributing to the pathogenesis of fibroproliferative disorders [150, 153, 154]. In our *in vivo* experiment, increased salt intake reduced the expression of *Il13* in the skin of IMQ-treated mice (Fig 7/g), which may contribute to the decreased Smad2/3 levels in the HSD IMQ group as well as to the diminished activation and ECM synthesis of DFs.

The thickness of the skin reflects to its collagen content, meaning that the accumulation of collagen in the skin is proportional to the cutaneous thickness and the extent of the scar tissue in dermal fibrosis [155-157]. Indeed, it has been demonstrated that excess collagen deposition is significantly increased in the dermis of patients with scleroderma, a fibroploriferative disease [157]. Our results showed that high salt diet reduced dermal thickness in mice treated with IMQ (Fig 10/f). The reduced skin thickness

in the HSD IMQ group is consistent with our results mentioned above demonstrating the inhibitory effect of high salt loading on expression of ECM components and related factors.

In the wound healing process, fibroblasts are the most prominent cell type, supporting collagen formation at the site of injury. After dynamic proliferation and ECM synthesis, ECM remodeling results in the development of a near-normal tissue architecture [92]. Since *in vivo* salt loading resulted in decreased ECM production, we hypothesize that high salt diet may lead to impaired dermal repair. Our hypothesis about the association between high salt diet and impaired wound healing is confirmed by the results of Binger et al. demonstrating delayed wound healing in mice on high salt diet [40]. However, their results suggest that decreased dermal M2 macrophage activity of mice kept on HSD is responsible for the delayed wound closure. In the event of wounding, macrophages are rapidly recruited to the site of injury, where M1 macrophages perform the initial proinflammatory response, followed by infiltration of anti-inflammatory M2 macrophages to heal and repair tissues.

We also investigated the effect of dietary salt overload on the dermal expression of matrix metalloproteinases, which are proteolytic enzymes with primary function to degrade collagens during ECM remodeling after injury, but their enzymatic activity also facilitates the inflammation via activation of inflammatory cytokines and chemokines [158]. Controlled degradation of the ECM is required to remove damaged components and to allow cell migration and angiogenesis. During the normal wound healing process, it is essential to restructure the ECM to allow cells to adhere and the basement membrane to be deposited. Previous experiments have shown the important role for MMPs in normal wound healing, but the rate and duration of MMP expression are limited and tightly controlled [159, 160]. Accordingly, MMPs are expressed at a low level in the healthy tissue, if at all [161]. However, our experiments demonstrated increased *Mmp2* and *Mmp9* expressions in the skin of mice on high salt diet (Fig 11/a,b). In chronic wounds, MMPs can lead to extensive tissue destruction and inhibit its regeneration. Several studies have confirmed a direct association between the increased expression of MMPs, primarily MMP-2 and MMP-9 in chronic wounds and delayed healing of chronic venous ulcers [162, 163]. Therefore, these results further support our above hypothesis that the increased salt intake may lead to ameliorated ECM remodeling of the skin.

Our *in vivo* results demonstrated that HSD influenced the expression of ECM components in the inflamed skin. Previous studies have shown that excessive salt intake increases the amount of both osmotically active and inactive Na^+ in the skin, as well as osmotic pressure, which can affect different cutaneous cell types [40, 50, 59]. Since dermal fibroblasts are the main sources of ECM components in the skin, our *in vitro* experiments focused on the effect of high salt loading on the functional activity of DFs. We found that 50 mM NaCl added to normal medium did not impair viability of DFs, did not cause cell death, and was consistent with the NaCl treatment used in the literature (Fig 9/a,b) [164, 165]. Therefore, in the *in vitro* experiments we kept the dermal fibroblasts in culture media supplemented with 50 mM NaCl to model the increased dermal Na^+ environment. The effect of increased NaCl concentration on cellular morphology was visualized by α-SMA immunofluorescence staining on the cytoskeleton of human DFs. Our results showed that the shape of the DFs became more circular in the high salt environment compared to that of control. (Fig 12/a). The shape of fibroblasts describes their migratory status. Circular DFs are in a stationary state, while the elongated shape suggests increased motility [166]. Indeed, due to the activity of the actin microfilaments, microtubules, and intermediate filaments involved in cell migration, the cell becomes polarized and the shape of the cell becomes elongated [104]. Therefore, the escalating circularity of high salt treated DFs indicates their reduced migration capacity. In addition to phenotypic changes, cell motility is also can be characterized by alterations of gene expression that alter the cytoskeleton structure thereby the motility of the cells. Indeed, the mRNA expression of fibroblast motility regulators VIM, VCL and ACTB decreased in the high salt treated group as well (Fig 12/b-d). Vimentin and vinculin are responsible for stabilizing cytoskeletal interactions and binding of cells to ECM elements, thereby supporting the migration of DFs to the site of injury [167]. Moreover, beta-actin is one of the major cellular cytoskeletal components that are involved in cell motility, which is largely driven by membrane protrusion forces resulting from the polymerization of beta-actin [168]. Consistent with these results, our *in vitro* TAS assay revealed a time-dependent decrease in migration capacity of DFs in high salt environment (Fig 12/e). Our results are consistent with previous results showing reduced migration capacity in high salt treated myocardial and endothelial cells [169, 170].

Since human dermal fibroblasts play a crucial role in wound contraction and healing through their ability to migrate, proliferate, and produce ECM, their decreased motility due to high salt loading presumably leads to impaired wound repairing mechanisms. Our *in vivo* results demonstrating decreased *Fn* and *Col1a1* expressions in the skin of IMQ treated mice on HSD (Fig 10/b,c), raised the question whether the dermal high salt environment has an effect on ECM production of dermal fibroblasts. Therefore, we investigated the effect of high salt loading on the ECM production of DFs. In line with the *in vivo* data, our *in vitro* experiments showed decreased endogenous *FN* and *COL1A1* expression, of DFs in high salt environment (Fig 13/a-c). In addition, FN and COL1A1 production induced by the profibrotic TGF-β was also inhibited by high salt condition (Fig 13/a-c). In essence, elevated local salt concentration could directly affect the ECM synthesis of dermal fibroblasts. These results could be explained by the previous results of our research group demonstrating that PGE2 production of DFs is enhanced after high salt loading, in addition, PGE2 has been shown to inhibit collagen expression of DFs via an autocrine TGF-β/Smad signaling pathway [31, 171].

In summary, according to our results, high salt loading and the consequently increased dermal sodium (Na^+) content reduced the expression of anti-inflammatory cytokines IL-10 and IL-13 by immune cells in the skin, even in dermatitis. These experimental data suggest the role of high salt intake in dermal inflammation. Moreover, our findings revealed the inhibitory effect of high salt concentration on the migration and ECM production of dermal fibroblast which can lead to impaired dermal ECM remodeling (Fig 17).

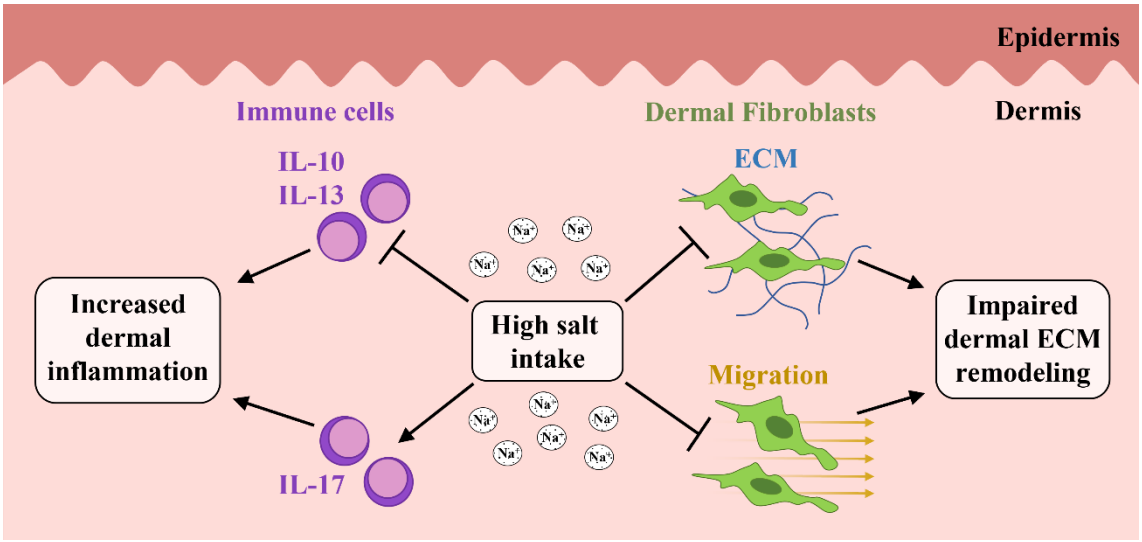

Figure 17. Schematic representation of the effect of excessive salt intake on mediating dermal inflammation and ECM remodeling.

(Szerkesztő program: Microsoft PowerPoint)

5.2 Transient Agarose Spot (TAS) assay: a new method to investigate cell migration

As fibroblast activity has been shown to play a role in the process of tissue fibrosis [79], it is important to develop test methods that can accurately examine the main properties of fibroblasts, such as migration capacity [88], proliferation [80] and ECM production [90]. The most frequently used growth factor to induce migration is the EGF[172, 173]. There are various well quantifiable assays to examine both fibroblast proliferation (e.g. thiazolyl blue tetrazolium bromide - MTT; bromodeoxyuridine - BrdU [105]), and ECM production (e.g. SiriusRed staining [106]), however the scratch assay is the most commonly used method for studying cell migration in two-dimensional monolayers (Fig 4) [174]. Although this assay has a number of advantages, including simplicity or affordability, it also has serious limitations that make it difficult to use it as a high-throughput tool [109]. Indeed, during scratch assay, the cell-free gap is manually generated by scratching the surface of a confluent cell monolayer using a pipette tip. Thereafter cell migration and gap closure kinetics are determined by graphical analysis. The main disadvantages of the scratch assay originate from the mechanical scratch itself, which damages the cells as well as the surface of the plate, which has a significant effect on cell motility [175]. Furthermore, scratching with the pipette tip results inconsistent initial gap size, which is reflected in the high intra- and inter-assay variability of the assay [174]. Instead of scratching, alternative methods to create a cell-free zone have recently been described, such as heat stamping, laser, electricity, enzymatic digestion, or vacuum [110, 176]. Most of these methods have similar defects, including damaged cells and surfaces, or result in gaps with irregular edges and sizes. In this regard, the use of pre-installed physical barriers where the cell-free zone is generated by plastic equipment or biocompatible gels may be a promising option [110-112]. However, these commercially available kits are very expensive and, like the scratch assay, mostly work with large surfaces (24 or 6 well plates) and thus large amounts of cells, reagents and compounds, resulting in a low-throughput technique instead of a high-throughput one [110].

Our newly developed transient agarose spot (TAS) assay eliminates the disadvantages of the above techniques using a simple, cost-effective, and high-throughput approach. In TAS assay, hydrogel drops of liquid agarose, which is a widely used, non-toxic, non-immunogenic biocompatible gel [177, 178], were placed in the center of the wells in a 96-well plate to exclude fibroblasts from a consistent, circular area (Fig 14/a).

Until the hydrogel drops were removed by pipetting, they remained stable in the center of the wells for numerous days despite cell manipulation (e.g., medium change, serum starvation, or even transfection). Nevertheless, after removal of the hydrogel drop, the fibroblasts began to migrate toward the cell-free surface of the gap, as indicated by a decrease in the initial size of the gap area (Fig 14/a, b).

Based on literature data, fibroblast migration can be stimulated by the addition of different profibrotic growth factors [108, 179, 180], as demonstrated by our experiments on EGF-treated fibroblasts (Fig 15/a, b). The high accuracy of the TAS assay allows the detection of migration differences even at an early stage of the experiment, up to 3 hours after the start of treatments (Fig 15/b). During the evaluation of the TAS assay data, cell migration is determined at certain intervals after taking serial images of the cell-free area. The gap areas can then be easily marked with graphical software (e.g. ImageJ) without any previous experience, and the size of the gap can be determined with a single measurement command.

After setting up the TAS assay, we compared its sensitivity and laboratory use with that of the gold standard scratch assay on EGF-stimulated fibroblasts (Fig 16). The benefits of the 96-well plate based TAS assay, in addition to its less raw material requirements, were immediately apparent. Indeed, the entire gap area fits into a single field of view of the microscope, allowing for easy automated documentation of the whole gap, reducing the need for human resources in the case of TAS assay (Fig 16/b). In contrast, in case of scratch assay, the process is more complex and identifying the same area at different time points is a real challenge [110]. In accordance with literature data, the standard deviation of the initial gap area was 3 times larger in the case of scratch compared to TAS assay (Fig 16/a) [108]. This is a serious limitation, as a larger standard deviation of the initial gap area may later result in an even higher standard deviation of the remaining cell-free gap area. Accordingly, although the kinetics of gap closure were similar in both assays, the TAS assay appeared to have significantly higher resolution, as evidenced by a 3-fold smaller deviation of the corresponding gap closure values compared to the scratch assay (Fig 16/c, d).

In summary, based on our comparative results, our newly developed TAS assay has more advantages in examining fibroblast migration than the scratch assay used as a gold standard in many ways. In addition to having the benefits of a scratch assay including

low material cost and simple technique, a consistent initial gap size and lower inter-assay variability can be achieved with TAS assay.

6. Conclusion

The salt consumption of modern societies far exceeds the recommendations of World Health Organization. Recent animal studies, as well as quantitative sodium MRI observations on humans demonstrated that remarkable amounts of sodium can be stored in the skin. It is also known that increased salt intake can induce inflammatory processes in various organs, but its role in dermal pathophysiology has not been elucidated. Our aim was therefore to study the effect of high salt loading on dermal inflammation and related extracellular matrix (ECM) remodeling. To investigate the effect of high salt consumption in the skin, mice were kept on normal (NSD) or high salt diet (HSD) and then a mouse model of imiquimod (IMQ) induced dermatitis was performed. The effect of high salt loading *in vitro* on dermal fibroblasts (DF) and peripheral blood mononuclear cells (PBMC) was also investigated. HSD resulted in increased dermal sodium concentrations in mice. The expression of the inflammatory cytokine *Il17* was increased in the skin of HSD mice. In addition, the anti-inflammatory *Il10* and *Il13* expressions were decreased in the skin of HSD or HSD IMQ mice. Expression of the fibroblast marker *Acta2* and the ECM component *Fn* and *Col1a1* was decreased in mice of HSD IMQ group. The level of ECM remodeling related *Pdgfb* and activation of phosphorylated (p)-SMAD2/3 was lower in HSD IMQ mice. Production of *IL10*, *IL13*, and *PDGFB* was also decreased in PBMCs due to high salt loading. In cultured DFs high salt concentration resulted in more circular morphology of DFs, decreased expression of cell motility regulators, including *VIM*, *VCL*, *ACTB* and decreased ECM production, as well. Our findings demonstrate that high salt diet is associated with increased inflammatory status of the skin. Although inflammation induces ECM synthesis in most organs, the expression of ECM components was decreased in the inflamed skin of mice on increased salt diet. Our results suggest that high dietary salt intake may alter the process of dermal tissue remodeling.

We also developed the so called transient agarose spot (TAS) migration assay, a new high throughput 96 well plate based method to study fibroblast migration in response to various stimuli. Our self-developed assay has several advantages over the most frequently used cell migration assays, including its accuracy, price, and high throughput property. Based on its advantages our assay may contribute to the fibrosis related basic research and identification of new anti-fibrotic compounds, as well.

7. Summary

The salt consumption of modern societies far exceeds the recommendations of World Health Organization. Our results showed that high salt diet leads to increased dermal sodium content thereby inducing pathological process, including inflammation and impaired dermal fibroblast activity. Therefore, our observations raise the possibility that high dietary salt intake can be considered as a potential risk factor for skin pathologies associated with inflammation and impaired wound healing.

We also developed a new cell migration assay which can be an improved alternative to the most frequently used scratch assay, retaining its advantages and eliminating most of its limitations. Since cell migration is a hallmark of tissue remodelling processes, including fibrosis, and wound healing, it is important to develop accurate cell migration test methods, that can be used to identify new potential anti-fibrotic compound.

8. References

1. Doyle, M.E. and K.A. Glass, *Sodium Reduction and Its Effect on Food Safety, Food Quality, and Human Health.* Comprehensive Reviews in Food Science and Food Safety, 2010. **9**(1): p. 44-56.
2. Strazzullo, P. and C. Leclercq, *Sodium.* Advances in nutrition (Bethesda, Md.), 2014. **5**(2): p. 188-190.
3. Afsar, B., M. Kuwabara, A. Ortiz, A. Yerlikaya, D. Siriopol, A. Covic, B. Rodriguez-Iturbe, R.J. Johnson and M. Kanbay, *Salt Intake and Immunity.* Hypertension, 2018. **72**(1): p. 19-23.
4. Costa, A.P.R., R.C.S. de Paula, G.F. Carvalho, J.P. Araújo, J.M. Andrade, O.L.R. de Almeida, E.C. de Faria, W.M. Freitas, O.R. Coelho, J.A.F. Ramires, J.C. Quinaglia e Silva and A.C. Sposito, *High sodium intake adversely affects oxidative-inflammatory response, cardiac remodelling and mortality after myocardial infarction.* Atherosclerosis, 2012. **222**(1): p. 284-291.
5. World Health, O., *Diet, nutrition and the prevention of chronic diseases : report of a joint WHO/FAO expert consultation, Geneva, 28 January - 1 February 2002*. 2003, World Health Organization: Geneva.
6. *Salt reduction*. 2020; Available from: https://www.who.int/news-room/fact-sheets/detail/salt-reduction.
7. Martos, É., M. Bakacs, E. Sarkadi-Nagy, T. Ráczkevy, A. Zentai, Z. Baldauf, É. Illés and A. Lugasi, *Hungarian Diet and Nutritional Status Survey – The OTAP2009 study. IV. Macroelement intake of the Hungarian population.* Orvosi Hetilap, 2012. **153**(29): p. 1132-1141.
8. *Global NCD Target, Reduce Salt Intake*. 2016; Available from: https://www.who.int/beat-ncds/take-action/policy-brief-reduce-salt-intake.pdf.
9. Knepper, M.A., T.-H. Kwon and S. Nielsen, *Molecular Physiology of Water Balance.* New England Journal of Medicine, 2015. **372**(14): p. 1349-1358.
10. Goetz, K.L., *Physiology and pathophysiology of atrial peptides.* American Journal of Physiology-Endocrinology and Metabolism, 1988. **254**(1): p. E1-E15.
11. Bankir, L., D.G. Bichet and N. Bouby, *Vasopressin V2 receptors, ENaC, and sodium reabsorption: a risk factor for hypertension?* American Journal of Physiology-Renal Physiology, 2010. **299**(5): p. F917-F928.

12. Elijovich, F., M.H. Weinberger, C.A.M. Anderson, L.J. Appel, M. Bursztyn, N.R. Cook, R.A. Dart, C.H. Newton-Cheh, F.M. Sacks and C.L. Laffer, *Salt Sensitivity of Blood Pressure.* Hypertension, 2016. **68**(3): p. e7-e46.
13. Bie, P., *Mechanisms of sodium balance: total body sodium, surrogate variables, and renal sodium excretion.* American Journal of Physiology-Regulatory, Integrative and Comparative Physiology, 2018. **315**(5): p. R945-R962.
14. Valtin H, S.J., *Renal Function: Mechanisms Preserving Fluid and Solute Balance in Health*. 1995: Boston: Little Brown.
15. Carruthers, C., *Biochemistry of skin in health and disease*. 1962, Springfield, Ill.: Thomas.
16. Eisele, C.W. and L. Eichelberger, *Water, Electrolyte and Nitrogen Content of Human Skin.* Proceedings of the Society for Experimental Biology and Medicine, 1945. **58**(1): p. 97-100.
17. Urbach, E. and E.B. Lewinn, *Skin diseases, nutrition and metabolism, Grune & Stratton.* Inc., New York, 1946: p. 23–24.
18. Wahlgren, V. and R. Magnus, *Über die Bedeutung der Gewebe als Chlordepots.* Archiv für experimentelle Pathologie und Pharmakologie, 1909. **61**(2): p. 97-112.
19. Jantsch, J., V. Schatz, D. Friedrich, A. Schröder, C. Kopp, I. Siegert, A. Maronna, D. Wendelborn, P. Linz, K.J. Binger, M. Gebhardt, M. Heinig, P. Neubert, F. Fischer, S. Teufel, J.P. David, C. Neufert, A. Cavallaro, N. Rakova, C. Küper, F.X. Beck, W. Neuhofer, D.N. Muller, G. Schuler, M. Uder, C. Bogdan, F.C. Luft and J. Titze, *Cutaneous Na+ storage strengthens the antimicrobial barrier function of the skin and boosts macrophage-driven host defense.* Cell Metab., 2015(1932-7420).
20. Machnik, A., J. Neuhofer W Fau - Jantsch, A. Jantsch J Fau - Dahlmann, T. Dahlmann A Fau - Tammela, K. Tammela T Fau - Machura, J.-K. Machura K Fau - Park, F.-X. Park Jk Fau - Beck, D.N. Beck Fx Fau - Müller, W. Müller Dn Fau - Derer, J. Derer W Fau - Goss, A. Goss J Fau - Ziomber, P. Ziomber A Fau - Dietsch, H. Dietsch P Fau - Wagner, N. Wagner H Fau - van Rooijen, A. van Rooijen N Fau - Kurtz, K.F. Kurtz A Fau - Hilgers, K. Hilgers Kf Fau - Alitalo, K.-U. Alitalo K Fau - Eckardt, F.C. Eckardt Ku Fau - Luft, D. Luft Fc Fau - Kerjaschki, J. Kerjaschki D Fau - Titze and J. Titze, *Macrophages regulate salt-*

dependent volume and blood pressure by a vascular endothelial growth factor-C-dependent buffering mechanism. Nat Med., 2009(1546-170X).

21. Nikpey, E., T.V. Karlsen, N. Rakova, J.M. Titze, O. Tenstad and H. Wiig, *High-Salt Diet Causes Osmotic Gradients and Hyperosmolality in Skin Without Affecting Interstitial Fluid and Lymph.* Hypertension, 2017(1524-4563).
22. Titze, J., C. Lang R Fau - Ilies, K.H. Ilies C Fau - Schwind, K.A. Schwind Kh Fau - Kirsch, P. Kirsch Ka Fau - Dietsch, F.C. Dietsch P Fau - Luft, K.F. Luft Fc Fau - Hilgers and K.F. Hilgers, *Osmotically inactive skin Na+ storage in rats.* Am J Physiol Renal Physiol., 2003(1931-857X).
23. Titze, J., M. Shakibaei M Fau - Schafflhuber, G. Schafflhuber M Fau - Schulze-Tanzil, M. Schulze-Tanzil G Fau - Porst, K.H. Porst M Fau - Schwind, P. Schwind Kh Fau - Dietsch, K.F. Dietsch P Fau - Hilgers and K.F. Hilgers, *Glycosaminoglycan polymerization may enable osmotically inactive Na+ storage in the skin.* Am J Physiol Heart Circ Physiol., 2004(0363-6135).
24. Wiig, H., T. Karlsen, O. Tenstad and J. Titze, *Increased interstitial osmolality in skin of rats on a high salt diet.* The FASEB Journal, 2013. **27**(S1): p. 680.2-680.2.
25. Wiig, H., W. Schröder A Fau - Neuhofer, J. Neuhofer W Fau - Jantsch, C. Jantsch J Fau - Kopp, T.V. Kopp C Fau - Karlsen, M. Karlsen Tv Fau - Boschmann, J. Boschmann M Fau - Goss, M. Goss J Fau - Bry, N. Bry M Fau - Rakova, A. Rakova N Fau - Dahlmann, S. Dahlmann A Fau - Brenner, O. Brenner S Fau - Tenstad, H. Tenstad O Fau - Nurmi, E. Nurmi H Fau - Mervaala, H. Mervaala E Fau - Wagner, F.-X. Wagner H Fau - Beck, D.N. Beck Fx Fau - Müller, D. Müller Dn Fau - Kerjaschki, F.C. Kerjaschki D Fau - Luft, D.G. Luft Fc Fau - Harrison, K. Harrison Dg Fau - Alitalo, J. Alitalo K Fau - Titze and J. Titze, *Immune cells control skin lymphatic electrolyte homeostasis and blood pressure.* J Clin Invest., 2013(1558-8238).
26. Aukland, K. and R.K. Reed, *Interstitial-lymphatic mechanisms in the control of extracellular fluid volume.* Physiological Reviews, 1993. **73**(1): p. 1-78.
27. Tobin, D.J., *Biochemistry of human skin—our brain on the outside.* Chemical Society Reviews, 2006. **35**(1): p. 52-67.
28. Goldsmith, L.A., *Physiology, biochemistry, and molecular biology of the skin*. Vol. 2. 1991: Oxford University Press.

29. Jackson, R.L., S.J. Busch and A.D. Cardin, *Glycosaminoglycans: molecular properties, protein interactions, and role in physiological processes.* Physiological Reviews, 1991. **71**(2): p. 481-539.
30. Fischereder, M., B. Michalke, E. Schmöckel, A. Habicht, R. Kunisch, I. Pavelic, B. Szabados, U. Schönermarck, P.J. Nelson and M. Stangl, *Sodium storage in human tissues is mediated by glycosaminoglycan expression.* American Journal of Physiology-Renal Physiology, 2017. **313**(2): p. F319-F325.
31. Agócs, R., D. Pap, D. Sugár, G. Tóth, L. Turiák, Z. Veréb, L. Kemény, T. Tulassay, Á. Vannay and A.J. Szabó, *Cyclooxygenase-2 Modulates Glycosaminoglycan Production in the Skin During Salt Overload.* Frontiers in physiology, 2020. **11**: p. 561722-561722.
32. Lopes-Menezes, V.C., R.C. Dos-Santos, V. Felintro, L.R.N. Monteiro, B. Paes-Leme, D. Lustrino, E.A. Casartelli, L. Vivas, A.S. Mecawi and L.C. Reis, *Acute body sodium depletion induces skin sodium mobilization in female Wistar rats.* Experimental Physiology, 2019. **104**(12): p. 1754-1761.
33. Schafflhuber, M., N. Volpi, A. Dahlmann, K.F. Hilgers, F. Maccari, P. Dietsch, H. Wagner, F.C. Luft, K.-U. Eckardt and J. Titze, *Mobilization of osmotically inactive Na+ by growth and by dietary salt restriction in rats.* American Journal of Physiology-Renal Physiology, 2007. **292**(5): p. F1490-F1500.
34. Sugár, D., E. Agócs R Fau - Tatár, G. Tatár E Fau - Tóth, P. Tóth G Fau - Horváth, E. Horváth P Fau - Sulyok, A.J. Sulyok E Fau - Szabó and A.J. Szabó, *The contribution of skin glycosaminoglycans to the regulation of sodium homeostasis in rats.* Physiol Res., 2018 (1802-9973 (Electronic)).
35. Olde Engberink, R.H.G., J. de Vos, A. van Weert, Y. Zhang, N. van Vlies, B.-J.H. van den Born, J.M. Titze, E. van Bavel and L. Vogt, *Abnormal sodium and water homeostasis in mice with defective heparan sulfate polymerization.* PLOS ONE, 2019. **14**(7): p. e0220333.
36. Titze, J., H. Krause, H. Hecht, P. Dietsch, J. Rittweger, R. Lang, K.A. Kirsch and K.F. Hilgers, *Reduced osmotically inactive Na storage capacity and hypertension in the Dahl model.* American Journal of Physiology-Renal Physiology, 2002. **283**(1): p. F134-F141.

37. Matthias, J., J. Maul, R. Noster, H. Meinl, Y.-Y. Chao, H. Gerstenberg, F. Jeschke, G. Gasparoni, A. Welle, J. Walter, K. Nordström, K. Eberhardt, D. Renisch, S. Donakonda, P. Knolle, D. Soll, S. Grabbe, N. Garzorz-Stark, K. Eyerich, T. Biedermann, D. Baumjohann and E. Zielinski Christina, *Sodium chloride is an ionic checkpoint for human TH2 cells and shapes the atopic skin microenvironment.* Science Translational Medicine, 2019. **11**(480): p. eaau0683.

38. Kleinewietfeld, M., A. Manzel, J. Titze, H. Kvakan, N. Yosef, R.A. Linker, D.N. Muller and D.A. Hafler, *Sodium chloride drives autoimmune disease by the induction of pathogenic TH17 cells.* Nature, 2013. **496**(7446): p. 518-522.

39. Kleinewietfeld, M., A. Manzel, C. Wu, J. Titze, V. Kuchroo, R. Linker, D. Muller and D. Hafler, *High salt induces pathogenic Th17 cells and exacerbates autoimmune diseases (60.13).* The Journal of Immunology, 2012. **188**(1 Supplement): p. 60.13.

40. Binger Kj Fau - Gebhardt, M., M. Gebhardt M Fau - Heinig, C. Heinig M Fau - Rintisch, A. Rintisch C Fau - Schroeder, W. Schroeder A Fau - Neuhofer, K. Neuhofer W Fau - Hilgers, A. Hilgers K Fau - Manzel, C. Manzel A Fau - Schwartz, M. Schwartz C Fau - Kleinewietfeld, J. Kleinewietfeld M Fau - Voelkl, V. Voelkl J Fau - Schatz, R.A. Schatz V Fau - Linker, F. Linker Ra Fau - Lang, D. Lang F Fau - Voehringer, M.D. Voehringer D Fau - Wright, N. Wright Md Fau - Hubner, R. Hubner N Fau - Dechend, J. Dechend R Fau - Jantsch, J. Jantsch J Fau - Titze, D.N. Titze J Fau - Müller and D.N. Müller, *High salt reduces the activation of IL-4- and IL-13-stimulated macrophages.* J Clin Invest., 2015(1558-8238).

41. Graudal, N.A., T. Hubeck-Graudal and G. Jurgens, *Effects of low sodium diet versus high sodium diet on blood pressure, renin, aldosterone, catecholamines, cholesterol, and triglyceride.* Cochrane Database of Systematic Reviews, 2017(4).

42. Juraschek, S.P., L.C. Kovell, L.J. Appel, E.R. Miller, F.M. Sacks, A.R. Chang, R.H. Christenson, H. Rebuck and K.J. Mukamal, *Effects of Diet and Sodium Reduction on Cardiac Injury, Strain, and Inflammation: The DASH-Sodium Trial.* Journal of the American College of Cardiology, 2021. **77**(21): p. 2625-2634.

43. Forouzanfar, M.H., L. Alexander, H.R. Anderson, V.F. Bachman, S. Biryukov, M. Brauer, R. Burnett, D. Casey, M.M. Coates, A. Cohen, K. Delwiche, K. Estep, J.J. Frostad, A. Kc, H.H. Kyu, M. Moradi-Lakeh, M. Ng, E.L. Slepak, B.A. Thomas, J. Wagner, G.M. Aasvang, C. Abbafati, A.A. Ozgoren, F. Abd-Allah, S.F. Abera, V. Aboyans, B. Abraham, J.P. Abraham, I. Abubakar, N.M.E. Abu-Rmeileh, T.C. Aburto, T. Achoki, A. Adelekan, K. Adofo, A.K. Adou, J.C. Adsuar, A. Afshin, E.E. Agardh, M.J. Al Khabouri, F.H. Al Lami, S.S. Alam, D. Alasfoor, M.I. Albittar, M.A. Alegretti, A.V. Aleman, Z.A. Alemu, R. Alfonso-Cristancho, S. Alhabib, R. Ali, M.K. Ali, F. Alla, P. Allebeck, P.J. Allen, U. Alsharif, E. Alvarez, N. Alvis-Guzman, A.A. Amankwaa, A.T. Amare, E.A. Ameh, O. Ameli, H. Amini, W. Ammar, B.O. Anderson, C.A.T. Antonio, P. Anwari, S.A. Cunningham, J. Arnlöv, V.S.A. Arsenijevic, A. Artaman, R.J. Asghar, R. Assadi, L.S. Atkins, C. Atkinson, M.A. Avila, B. Awuah, A. Badawi, M.C. Bahit, T. Bakfalouni, K. Balakrishnan, S. Balalla, R.K. Balu, A. Banerjee, R.M. Barber, S.L. Barker-Collo, S. Barquera, L. Barregard, L.H. Barrero, T. Barrientos-Gutierrez, A.C. Basto-Abreu, A. Basu, S. Basu, M.O. Basulaiman, C.B. Ruvalcaba, J. Beardsley, N. Bedi, T. Bekele, M.L. Bell, C. Benjet, D.A. Bennett, H. Benzian, E. Bernabé, T.J. Beyene, N. Bhala, A. Bhalla, Z.A. Bhutta, B. Bikbov, A.A.B. Abdulhak, J.D. Blore, F.M. Blyth, M.A. Bohensky, B.B. Başara, G. Borges, N.M. Bornstein, D. Bose, S. Boufous, R.R. Bourne, M. Brainin, A. Brazinova, N.J. Breitborde, H. Brenner, A.D.M. Briggs, D.M. Broday, P.M. Brooks, N.G. Bruce, T.S. Brugha, B. Brunekreef, R. Buchbinder, L.N. Bui, G. Bukhman, A.G. Bulloch, M. Burch, P.G.J. Burney, I.R. Campos-Nonato, J.C. Campuzano, A.J. Cantoral, J. Caravanos, R. Cárdenas, E. Cardis, D.O. Carpenter, V. Caso, C.A. Castañeda-Orjuela, R.E. Castro, F. Catalá-López, F. Cavalleri, A. Çavlin, V.K. Chadha, J.-c. Chang, F.J. Charlson, H. Chen, W. Chen, Z. Chen, P.P. Chiang, O. Chimed-Ochir, R. Chowdhury, C.A. Christophi, T.-W. Chuang, S.S. Chugh, M. Cirillo, T.K.D. Claßen, V. Colistro, M. Colomar, S.M. Colquhoun, A.G. Contreras, C. Cooper, K. Cooperrider, L.T. Cooper, J. Coresh, K.J. Courville, M.H. Criqui, L. Cuevas-Nasu, J. Damsere-Derry, H. Danawi, L. Dandona, R. Dandona, P.I. Dargan, A. Davis, D.V. Davitoiu, A. Dayama, E.F. de Castro, V. De la Cruz-Góngora, D. De Leo, G. de Lima, L. Degenhardt, B. del

Pozo-Cruz, R.P. Dellavalle, K. Deribe, S. Derrett, D.C.D. Jarlais, M. Dessalegn, G.A. deVeber, K.M. Devries, S.D. Dharmaratne, M.K. Dherani, D. Dicker, E.L. Ding, K. Dokova, E.R. Dorsey, T.R. Driscoll, L. Duan, A.M. Durrani, B.E. Ebel, R.G. Ellenbogen, Y.M. Elshrek, M. Endres, S.P. Ermakov, H.E. Erskine, B. Eshrati, A. Esteghamati, S. Fahimi, E.J.A. Faraon, F. Farzadfar, D.F.J. Fay, V.L. Feigin, A.B. Feigl, S.-M. Fereshtehnejad, A.J. Ferrari, C.P. Ferri, A.D. Flaxman, T.D. Fleming, N. Foigt, K.J. Foreman, U.F. Paleo, R.C. Franklin, B. Gabbe, L. Gaffikin, E. Gakidou, A. Gamkrelidze, F.G. Gankpé, R.T. Gansevoort, F.A. García-Guerra, E. Gasana, J.M. Geleijnse, B.D. Gessner, P. Gething, K.B. Gibney, R.F. Gillum, I.A.M. Ginawi, M. Giroud, G. Giussani, S. Goenka, K. Goginashvili, H.G. Dantes, P. Gona, T.G. de Cosio, D. González-Castell, C.C. Gotay, A. Goto, H.N. Gouda, R.L. Guerrant, H.C. Gugnani, F. Guillemin, D. Gunnell, R. Gupta, R. Gupta, R.A. Gutiérrez, N. Hafezi-Nejad, H. Hagan, M. Hagstromer, Y.A. Halasa, R.R. Hamadeh, M. Hammami, G.J. Hankey, Y. Hao, H.L. Harb, T.N. Haregu, J.M. Haro, R. Havmoeller, S.I. Hay, M.T. Hedayati, I.B. Heredia-Pi, L. Hernandez, K.R. Heuton, P. Heydarpour, M. Hijar, H.W. Hoek, H.J. Hoffman, J.C. Hornberger, H.D. Hosgood, D.G. Hoy, M. Hsairi, G. Hu, H. Hu, C. Huang, J.J. Huang, B.J. Hubbell, L. Huiart, A. Husseini, M.L. Iannarone, K.M. Iburg, B.T. Idrisov, N. Ikeda, K. Innos, M. Inoue, F. Islami, S. Ismayilova, K.H. Jacobsen, H.A. Jansen, D.L. Jarvis, S.K. Jassal, A. Jauregui, S. Jayaraman, P. Jeemon, P.N. Jensen, V. Jha, F. Jiang, G. Jiang, Y. Jiang, J.B. Jonas, K. Juel, H. Kan, S.S.K. Roseline, N.E. Karam, A. Karch, C.K. Karema, G. Karthikeyan, A. Kaul, N. Kawakami, D.S. Kazi, A.H. Kemp, A.P. Kengne, A. Keren, Y.S. Khader, S.E.A.H. Khalifa, E.A. Khan, Y.-H. Khang, S. Khatibzadeh, I. Khonelidze, C. Kieling, D. Kim, S. Kim, Y. Kim, R.W. Kimokoti, Y. Kinfu, J.M. Kinge, B.M. Kissela, M. Kivipelto, L.D. Knibbs, A.K. Knudsen, Y. Kokubo, M.R. Kose, S. Kosen, A. Kraemer, M. Kravchenko, S. Krishnaswami, H. Kromhout, T. Ku, B.K. Defo, B.K. Bicer, E.J. Kuipers, C. Kulkarni, V.S. Kulkarni, G.A. Kumar, G.F. Kwan, T. Lai, A.L. Balaji, R. Lalloo, T. Lallukka, H. Lam, Q. Lan, V.C. Lansingh, H.J. Larson, A. Larsson, D.O. Laryea, P.M. Lavados, A.E. Lawrynowicz, J.L. Leasher, J.-T. Lee, J. Leigh, R. Leung, M. Levi, Y. Li, Y. Li, J. Liang, X. Liang, S.S. Lim, M.P. Lindsay, S.E. Lipshultz, S. Liu, Y. Liu, B.K.

Lloyd, G. Logroscino, S.J. London, N. Lopez, J. Lortet-Tieulent, P.A. Lotufo, R. Lozano, R. Lunevicius, J. Ma, S. Ma, V.M.P. Machado, M.F. MacIntyre, C. Magis-Rodriguez, A.A. Mahdi, M. Majdan, R. Malekzadeh, S. Mangalam, C.C. Mapoma, M. Marape, W. Marcenes, D.J. Margolis, C. Margono, G.B. Marks, R.V. Martin, M.B. Marzan, M.T. Mashal, F. Masiye, A.J. Mason-Jones, K. Matsushita, R. Matzopoulos, B.M. Mayosi, T.T. Mazorodze, A.C. McKay, M. McKee, A. McLain, P.A. Meaney, C. Medina, M.M. Mehndiratta, F. Mejia-Rodriguez, W. Mekonnen, Y.A. Melaku, M. Meltzer, Z.A. Memish, W. Mendoza, G.A. Mensah, A. Meretoja, F.A. Mhimbira, R. Micha, T.R. Miller, E.J. Mills, A. Misganaw, S. Mishra, N.M. Ibrahim, K.A. Mohammad, A.H. Mokdad, G.L. Mola, L. Monasta, J.C.M. Hernandez, M. Montico, A.R. Moore, L. Morawska, R. Mori, J. Moschandreas, W.N. Moturi, D. Mozaffarian, U.O. Mueller, M. Mukaigawara, E.C. Mullany, K.S. Murthy, M. Naghavi, Z. Nahas, A. Naheed, K.S. Naidoo, L. Naldi, D. Nand, V. Nangia, K.M.V. Narayan, D. Nash, B. Neal, C. Nejjari, S.P. Neupane, C.R. Newton, F.N. Ngalesoni, J. de Dieu Ngirabega, G. Nguyen, N.T. Nguyen, M.J. Nieuwenhuijsen, M.I. Nisar, J.R. Nogueira, J.M. Nolla, S. Nolte, O.F. Norheim, R.E. Norman, B. Norrving, L. Nyakarahuka, I.-H. Oh, T. Ohkubo, B.O. Olusanya, S.B. Omer, J.N. Opio, R. Orozco, R.S. Pagcatipunan, Jr., A.W. Pain, J.D. Pandian, C.I.A. Panelo, C. Papachristou, E.-K. Park, C.D. Parry, A.J.P. Caicedo, S.B. Patten, V.K. Paul, B.I. Pavlin, N. Pearce, L.S. Pedraza, A. Pedroza, L.P. Stokic, A. Pekericli, D.M. Pereira, R. Perez-Padilla, F. Perez-Ruiz, N. Perico, S.A.L. Perry, A. Pervaiz, K. Pesudovs, C.B. Peterson, M. Petzold, M.R. Phillips, H.P. Phua, D. Plass, D. Poenaru, G.V. Polanczyk, S. Polinder, C.D. Pond, C.A. Pope, D. Pope, S. Popova, F. Pourmalek, J. Powles, D. Prabhakaran, N.M. Prasad, D.M. Qato, A.D. Quezada, D.A.A. Quistberg, L. Racapé, A. Rafay, K. Rahimi, V. Rahimi-Movaghar, S.U. Rahman, M. Raju, I. Rakovac, S.M. Rana, M. Rao, H. Razavi, K.S. Reddy, A.H. Refaat, J. Rehm, G. Remuzzi, A.L. Ribeiro, P.M. Riccio, L. Richardson, A. Riederer, M. Robinson, A. Roca, A. Rodriguez, D. Rojas-Rueda, I. Romieu, L. Ronfani, R. Room, N. Roy, G.M. Ruhago, L. Rushton, N. Sabin, R.L. Sacco, S. Saha, R. Sahathevan, M.A. Sahraian, J.A. Salomon, D. Salvo, U.K. Sampson, J.R. Sanabria, L.M. Sanchez, T.G. Sánchez-Pimienta, L. Sanchez-Riera, L. Sandar,

I.S. Santos, A. Sapkota, M. Satpathy, J.E. Saunders, M. Sawhney, M.I. Saylan, P. Scarborough, J.C. Schmidt, I.J.C. Schneider, B. Schöttker, D.C. Schwebel, J.G. Scott, S. Seedat, S.G. Sepanlou, B. Serdar, E.E. Servan-Mori, G. Shaddick, S. Shahraz, T.S. Levy, S. Shangguan, J. She, S. Sheikhbahaei, K. Shibuya, H.H. Shin, Y. Shinohara, R. Shiri, K. Shishani, I. Shiue, I.D. Sigfusdottir, D.H. Silberberg, E.P. Simard, S. Sindi, A. Singh, G.M. Singh, J.A. Singh, V. Skirbekk, K. Sliwa, M. Soljak, S. Soneji, K. Søreide, S. Soshnikov, L.A. Sposato, C.T. Sreeramareddy, N.J.C. Stapelberg, V. Stathopoulou, N. Steckling, D.J. Stein, M.B. Stein, N. Stephens, H. Stöckl, K. Straif, K. Stroumpoulis, L. Sturua, B.F. Sunguya, S. Swaminathan, M. Swaroop, B.L. Sykes, K.M. Tabb, K. Takahashi, R.T. Talongwa, N. Tandon, D. Tanne, M. Tanner, M. Tavakkoli, B.J. Te Ao, C.M. Teixeira, M.M. Téllez Rojo, A.S. Terkawi, J.L. Texcalac-Sangrador, S.V. Thackway, B. Thomson, A.L. Thorne-Lyman, A.G. Thrift, G.D. Thurston, T. Tillmann, M. Tobollik, M. Tonelli, F. Topouzis, J.A. Towbin, H. Toyoshima, J. Traebert, B.X. Tran, L. Trasande, M. Trillini, U. Trujillo, Z.T. Dimbuene, M. Tsilimbaris, E.M. Tuzcu, U.S. Uchendu, K.N. Ukwaja, S.B. Uzun, S. van de Vijver, R. Van Dingenen, C.H. van Gool, J. van Os, Y.Y. Varakin, T.J. Vasankari, A.M.N. Vasconcelos, M.S. Vavilala, L.J. Veerman, G. Velasquez-Melendez, N. Venketasubramanian, L. Vijayakumar, S. Villalpando, F.S. Violante, V.V. Vlassov, S.E. Vollset, G.R. Wagner, S.G. Waller, M.T. Wallin, X. Wan, H. Wang, J. Wang, L. Wang, W. Wang, Y. Wang, T.S. Warouw, C.H. Watts, S. Weichenthal, E. Weiderpass, R.G. Weintraub, A. Werdecker, K.R. Wessells, R. Westerman, H.A. Whiteford, J.D. Wilkinson, H.C. Williams, T.N. Williams, S.M. Woldeyohannes, C.D.A. Wolfe, J.Q. Wong, A.D. Woolf, J.L. Wright, B. Wurtz, G. Xu, L.L. Yan, G. Yang, Y. Yano, P. Ye, M. Yenesew, G.K. Yentür, P. Yip, N. Yonemoto, S.-J. Yoon, M.Z. Younis, Z. Younoussi, C. Yu, M.E. Zaki, Y. Zhao, Y. Zheng, M. Zhou, J. Zhu, S. Zhu, X. Zou, J.R. Zunt, A.D. Lopez, T. Vos and C.J. Murray, *Global, regional, and national comparative risk assessment of 79 behavioural, environmental and occupational, and metabolic risks or clusters of risks in 188 countries, 1990–2013: a systematic analysis for the Global Burden of Disease Study 2013.* The Lancet, 2015. **386**(10010): p. 2287-2323.

44. Kearney, P.M., M. Whelton, K. Reynolds, P. Muntner, P.K. Whelton and J. He, *Global burden of hypertension: analysis of worldwide data.* The Lancet, 2005. **365**(9455): p. 217-223.
45. Lawes, C.M.M., S.V. Hoorn and A. Rodgers, *Global burden of blood-pressure-related disease, 2001.* The Lancet, 2008. **371**(9623): p. 1513-1518.
46. Müller, D.A.-O., N. Wilck, S. Haase, M.A.-O. Kleinewietfeld and R.A. Linker, *Sodium in the microenvironment regulates immune responses and tissue homeostasis.* Nat Rev Immunol., 2019(1474-1741).
47. Wilck, N., A. Balogh, L. Markó, H. Bartolomaeus and D.N. Müller, *The role of sodium in modulating immune cell function.* Nature Reviews Nephrology, 2019. **15**(9): p. 546-558.
48. Chen, W., D. Pilling and R.H. Gomer, *Dietary NaCl affects bleomycin-induced lung fibrosis in mice.* Experimental lung research, 2017. **43**(9-10): p. 395-406.
49. Zhang, W.-C., L.-J. Du, X.-J. Zheng, X.-Q. Chen, C. Shi, B.-Y. Chen, X.-N. Sun, C. Li, Y.-Y. Zhang, Y. Liu, H. Xiao, Q. Leng, X. Jiang, Z. Zhang, S. Sun and S.-Z. Duan, *Elevated sodium chloride drives type I interferon signaling in macrophages and increases antiviral resistance.* The Journal of biological chemistry, 2018. **293**(3): p. 1030-1039.
50. Zhang, W.-C., X.-J. Zheng, L.-J. Du, J.-Y. Sun, Z.-X. Shen, C. Shi, S. Sun, Z. Zhang, X.-Q. Chen, M. Qin, X. Liu, J. Tao, L. Jia, H.-Y. Fan, B. Zhou, Y. Yu, H. Ying, L. Hui, X. Liu, X. Yi, X. Liu, L. Zhang and S.-Z. Duan, *High salt primes a specific activation state of macrophages, M(Na).* Cell research, 2015. **25**(8): p. 893-910.
51. Barbaro, N.R., J.D. Foss, D.O. Kryshtal, N. Tsyba, S. Kumaresan, L. Xiao, R.L. Mernaugh, H.A. Itani, R. Loperena, W. Chen, S. Dikalov, J.M. Titze, B.C. Knollmann, D.G. Harrison and A. Kirabo, *Dendritic Cell Amiloride-Sensitive Channels Mediate Sodium-Induced Inflammation and Hypertension.* Cell reports, 2017. **21**(4): p. 1009-1020.
52. Berry, M.R., R.J. Mathews, J.R. Ferdinand, C. Jing, K.W. Loudon, E. Wlodek, T.W. Dennison, C. Kuper, W. Neuhofer and M.R. Clatworthy, *Renal Sodium Gradient Orchestrates a Dynamic Antibacterial Defense Zone.* Cell., 2017(1097-4172).

53. Itani, H.A., L. Xiao, M.A. Saleh, J. Wu, M.A. Pilkinton, B.L. Dale, N.R. Barbaro, J.D. Foss, A. Kirabo, K.R. Montaniel, A.E. Norlander, W. Chen, R. Sato, L.G. Navar, S.A. Mallal, M.S. Madhur, K.E. Bernstein and D.G. Harrison, *CD70 Exacerbates Blood Pressure Elevation and Renal Damage in Response to Repeated Hypertensive Stimuli.* Circulation research, 2016. **118**(8): p. 1233-1243.
54. Aguiar, S.L.F., M.C.G. Miranda, M.A.F. Guimarães, H.C. Santiago, C.P. Queiroz, P.d.S. Cunha, D.C. Cara, G. Foureaux, A.J. Ferreira, V.N. Cardoso, P.A. Barros, T.U. Maioli and A.M.C. Faria, *High-Salt Diet Induces IL-17-Dependent Gut Inflammation and Exacerbates Colitis in Mice.* Frontiers in immunology, 2018. **8**: p. 1969-1969.
55. Monteleone, I., I. Marafini, V. Dinallo, D. Di Fusco, E. Troncone, F. Zorzi, F. Laudisi and G. Monteleone, *Sodium chloride–enriched Diet Enhanced Inflammatory Cytokine Production and Exacerbated Experimental Colitis in Mice.* Journal of Crohn's and Colitis, 2017. **11**(2): p. 237-245.
56. Tubbs, A.L., B. Liu, T.D. Rogers, R.B. Sartor and E.A. Miao, *Dietary Salt Exacerbates Experimental Colitis.* Journal of immunology (Baltimore, Md. : 1950), 2017. **199**(3): p. 1051-1059.
57. Wei, Y., C. Lu, J. Chen, G. Cui, L. Wang, T. Yu, Y. Yang, W. Wu, Y. Ding, L. Li, T. Uede, Z. Chen and H. Diao, *High salt diet stimulates gut Th17 response and exacerbates TNBS-induced colitis in mice.* Oncotarget, 2017. **8**(1): p. 70-82.
58. Selvarajah, V., K. Connolly, C. McEniery and I. Wilkinson, *Skin Sodium and Hypertension: a Paradigm Shift?* Current Hypertension Reports, 2018. **20**(11): p. 94.
59. Wu, C., N. Yosef, T. Thalhamer, C. Zhu, S. Xiao, Y. Kishi, A. Regev and V.K. Kuchroo, *Induction of pathogenic TH17 cells by inducible salt-sensing kinase SGK1.* Nature, 2013. **496**(7446): p. 513-517.
60. Korn, T., E. Bettelli, M. Oukka and V.K. Kuchroo, *IL-17 and Th17 Cells.* Annual Review of Immunology, 2009. **27**(1): p. 485-517.
61. Chiricozzi, A., E. Guttman-Yassky, M. Suárez-Fariñas, K.E. Nograles, S. Tian, I. Cardinale, S. Chimenti and J.G. Krueger, *Integrative Responses to IL-17 and TNF-α in Human Keratinocytes Account for Key Inflammatory Pathogenic*

Circuits in Psoriasis. Journal of Investigative Dermatology, 2011. **131**(3): p. 677-687.

62. Miossec, P., T. Korn and V.K. Kuchroo, *Interleukin-17 and Type 17 Helper T Cells.* New England Journal of Medicine, 2009. **361**(9): p. 888-898.
63. Bettelli, E., Y. Carrier, W. Gao, T. Korn, T.B. Strom, M. Oukka, H.L. Weiner and V.K. Kuchroo, *Reciprocal developmental pathways for the generation of pathogenic effector TH17 and regulatory T cells.* Nature, 2006. **441**(7090): p. 235-238.
64. Mailer, R.K.W., A.-L. Joly, S. Liu, S. Elias, J. Tegner and J. Andersson, *IL-1β promotes Th17 differentiation by inducing alternative splicing of FOXP3.* Scientific Reports, 2015. **5**(1): p. 14674.
65. Veldhoen, M., R.J. Hocking, C.J. Atkins, R.M. Locksley and B. Stockinger, *TGFβ in the Context of an Inflammatory Cytokine Milieu Supports De Novo Differentiation of IL-17-Producing T Cells.* Immunity, 2006. **24**(2): p. 179-189.
66. Zhao, C., Y. Gu, X. Zeng and J. Wang, *NLRP3 inflammasome regulates Th17 differentiation in rheumatoid arthritis.* Clinical Immunology, 2018. **197**: p. 154-160.
67. Zheng, Y., L. Sun, T. Jiang, D. Zhang, D. He and H. Nie, *TNFα Promotes Th17 Cell Differentiation through IL-6 and IL-1β Produced by Monocytes in Rheumatoid Arthritis.* Journal of Immunology Research, 2014. **2014**: p. 385352.
68. Guo, B., *IL-10 Modulates Th17 Pathogenicity during Autoimmune Diseases.* Journal of clinical & cellular immunology, 2016. **7**(2): p. 400.
69. Huber, S., N. Gagliani, E. Esplugues, W. O'Connor, Jr., F.J. Huber, A. Chaudhry, M. Kamanaka, Y. Kobayashi, C.J. Booth, A.Y. Rudensky, M.G. Roncarolo, M. Battaglia and R.A. Flavell, *Th17 cells express interleukin-10 receptor and are controlled by Foxp3⁻ and Foxp3+ regulatory CD4+ T cells in an interleukin-10-dependent manner.* Immunity, 2011. **34**(4): p. 554-565.
70. Newcomb, D.C., M.G. Boswell, M.M. Huckabee, K. Goleniewska, D.E. Dulek, S. Reiss, N.W. Lukacs, J.K. Kolls and R.S. Peebles, Jr., *IL-13 regulates Th17 secretion of IL-17A in an IL-10-dependent manner.* Journal of immunology (Baltimore, Md. : 1950), 2012. **188**(3): p. 1027-1035.

71. Hucke, S., M. Eschborn, M. Liebmann, M. Herold, N. Freise, A. Engbers, P. Ehling, S.G. Meuth, J. Roth, T. Kuhlmann, H. Wiendl and L. Klotz, *Sodium chloride promotes pro-inflammatory macrophage polarization thereby aggravating CNS autoimmunity.* Journal of Autoimmunity, 2016. **67**: p. 90-101.
72. Luo, T., W.-j. Ji, F. Yuan, Z.-z. Guo, Y.-x. Li, Y. Dong, Y.-q. Ma, X. Zhou and Y.-m. Li, *Th17/Treg Imbalance Induced by Dietary Salt Variation Indicates Inflammation of Target Organs in Humans.* Scientific Reports, 2016. **6**(1): p. 26767.
73. Pitzer, A.L., N.R. Barbaro, L. Aden, E.C. Ray, T.R. Kleyman and A. Kirabo, *Abstract MP38: High Salt Activates The NLRP3 Inflammasome In Antigen Presenting Cells Via ENaC To Promote Salt-Sensitive Hypertension.* Hypertension, 2020. **76**(Suppl_1): p. AMP38-AMP38.
74. Yi, B., J. Titze, M. Rykova, M. Feuerecker, G. Vassilieva, I. Nichiporuk, G. Schelling, B. Morukov and A. Choukèr, *Effects of dietary salt levels on monocytic cells and immune responses in healthy human subjects: a longitudinal study.* Translational Research, 2015. **166**(1): p. 103-110.
75. Bubna, A.K., *Imiquimod - Its role in the treatment of cutaneous malignancies.* Indian journal of pharmacology, 2015. **47**(4): p. 354-359.
76. Sauder, D.N., *Imiquimod: modes of action.* British Journal of Dermatology, 2003. **149**(s66): p. 5-8.
77. Walter, A., M. Schäfer, V. Cecconi, C. Matter, M. Urosevic-Maiwald, B. Belloni, N. Schönewolf, R. Dummer, W. Bloch, S. Werner, H.-D. Beer, A. Knuth and M. van den Broek, *Aldara activates TLR7-independent immune defence.* Nature Communications, 2013. **4**(1): p. 1560.
78. van der Fits, L., S. Mourits, J.S.A. Voerman, M. Kant, L. Boon, J.D. Laman, F. Cornelissen, A.-M. Mus, E. Florencia, E.P. Prens and E. Lubberts, *Imiquimod-Induced Psoriasis-Like Skin Inflammation in Mice Is Mediated via the IL-23/IL-17 Axis.* The Journal of Immunology, 2009. **182**(9): p. 5836.
79. Pinet, K. and K.A. McLaughlin, *Mechanisms of physiological tissue remodeling in animals: Manipulating tissue, organ, and organism morphology.* Developmental Biology, 2019. **451**(2): p. 134-145.

80. Wynn, T.A., *Cellular and molecular mechanisms of fibrosis.* The Journal of pathology, 2008. **214**(2): p. 199-210.
81. Wynn, T.A., *Common and unique mechanisms regulate fibrosis in various fibroproliferative diseases.* The Journal of clinical investigation, 2007. **117**(3): p. 524-529.
82. Jun, J.-I. and L.F. Lau, *Resolution of organ fibrosis.* The Journal of Clinical Investigation, 2018. **128**(1): p. 97-107.
83. Lu, C.-Y. and S.-C. Lai, *Matrix metalloproteinase-2 and -9 lead to fibronectin degradation in astroglia infected with Toxoplasma gondii.* Acta Tropica, 2013. **125**(3): p. 320-329.
84. Webb, A.H., B.T. Gao, Z.K. Goldsmith, A.S. Irvine, N. Saleh, R.P. Lee, J.B. Lendermon, R. Bheemreddy, Q. Zhang, R.C. Brennan, D. Johnson, J.J. Steinle, M.W. Wilson and V.M. Morales-Tirado, *Inhibition of MMP-2 and MMP-9 decreases cellular migration, and angiogenesis in in vitro models of retinoblastoma.* BMC Cancer, 2017. **17**(1): p. 434.
85. Sorg, H., D.J. Tilkorn, S. Hager, J. Hauser and U. Mirastschijski, *Skin Wound Healing: An Update on the Current Knowledge and Concepts.* European Surgical Research, 2017. **58**(1-2): p. 81-94.
86. desJardins-Park, H.E., D.S. Foster and M.T. Longaker, *Fibroblasts and wound healing: an update.* Regenerative Medicine, 2018. **13**(5): p. 491-495.
87. Hinz, B., *Formation and Function of the Myofibroblast during Tissue Repair*. Journal of Investigative Dermatology, 2007. **127**(3): p. 526-537.
88. McDougall, S., J. Dallon, J. Sherratt and P. Maini, *Fibroblast migration and collagen deposition during dermal wound healing: mathematical modelling and clinical implications.* Philosophical Transactions of the Royal Society A: Mathematical, Physical and Engineering Sciences, 2006. **364**(1843): p. 1385-1405.
89. Britannica, T.E.o.E., *fibroblast.* Encyclopedia Britannica, 2018.
90. Dick MK, M.J., Limaiem F., *Histology, Fibroblast.* 2021 StatPearls Publishing, Treasure Island (FL).
91. Darby, I.A. and T.D. Hewitson, *Fibroblast Differentiation in Wound Healing and Fibrosis*, in *International Review of Cytology*. 2007, Academic Press. p. 143-179.

92. Gosain, A. and L.A. DiPietro, *Aging and Wound Healing.* World Journal of Surgery, 2004. **28**(3): p. 321-326.
93. Tripoli, M., A. Cordova and F. Moschella, *Update on the role of molecular factors and fibroblasts in the pathogenesis of Dupuytren's disease.* Journal of Cell Communication and Signaling, 2016. **10**(4): p. 315-330.
94. Wells, R.G., *Tissue mechanics and fibrosis.* Biochimica et Biophysica Acta (BBA) - Molecular Basis of Disease, 2013. **1832**(7): p. 884-890.
95. Walton, K.L., K.E. Johnson and C.A. Harrison, *Targeting TGF-β Mediated SMAD Signaling for the Prevention of Fibrosis.* Frontiers in Pharmacology, 2017. **8**.
96. Andrae, J., R. Gallini and C. Betsholtz, *Role of platelet-derived growth factors in physiology and medicine.* Genes & development, 2008. **22**(10): p. 1276-1312.
97. Joseph, R., O.P. Srivastava and R.R. Pfister, *Downregulation of β-actin and its regulatory gene HuR affect cell migration of human corneal fibroblasts.* Molecular vision, 2014. **20**: p. 593-605.
98. Rosowski, K.A., R. Boltyanskiy, Y. Xiang, K. Van den Dries, M.A. Schwartz and E.R. Dufresne, *Vinculin and the mechanical response of adherent fibroblasts to matrix deformation.* Scientific Reports, 2018. **8**(1): p. 17967.
99. Sliogeryte, K. and N. Gavara, *Vimentin Plays a Crucial Role in Fibroblast Ageing by Regulating Biophysical Properties and Cell Migration.* Cells, 2019. **8**(10): p. 1164.
100. Bretscher, M.S., *Getting Membrane Flow and the Cytoskeleton to Cooperate in Moving Cells.* Cell, 1996. **87**(4): p. 601-606.
101. Doherty, G.J. and H.T. McMahon, *Mediation, Modulation, and Consequences of Membrane-Cytoskeleton Interactions.* Annual Review of Biophysics, 2008. **37**(1): p. 65-95.
102. Pollard, T.D. and G.G. Borisy, *Cellular Motility Driven by Assembly and Disassembly of Actin Filaments.* Cell, 2003. **112**(4): p. 453-465.
103. Wang, Y.L., *Exchange of actin subunits at the leading edge of living fibroblasts: possible role of treadmilling.* Journal of Cell Biology, 1985. **101**(2): p. 597-602.
104. Seetharaman, S. and S. Etienne-Manneville, *Cytoskeletal Crosstalk in Cell Migration.* Trends in Cell Biology, 2020. **30**(9): p. 720-735.

105. Vega-Avila, E. and M.K. Pugsley, *An overview of colorimetric assay methods used to assess survival or proliferation of mammalian cells.* Proc West Pharmacol Soc., 2011(0083-8969 (Print)).
106. Chen, C.Z.C. and M. Raghunath, *Focus on collagen: in vitro systems to study fibrogenesis and antifibrosis _ state of the art.* Fibrogenesis & Tissue Repair, 2009. **2**(1): p. 7.
107. Justus, C.R., N. Leffler, M. Ruiz-Echevarria and L.V. Yang, *In vitro cell migration and invasion assays.* Journal of visualized experiments : JoVE, 2014(88): p. 51046.
108. Pijuan, J., C. Barceló, D.F. Moreno, O. Maiques, P. Sisó, R.M. Marti, A. Macià and A. Panosa, *In vitro Cell Migration, Invasion, and Adhesion Assays: From Cell Imaging to Data Analysis.* Frontiers in Cell and Developmental Biology, 2019. **7**.
109. Grada, A., M. Otero-Vinas, F. Prieto-Castrillo, Z. Obagi and V. Falanga, *Research Techniques Made Simple: Analysis of Collective Cell Migration Using the Wound Healing Assay.* Journal of Investigative Dermatology, 2017. **137**(2): p. e11-e16.
110. De Ieso, Michael L. and Jinxin V. Pei, *An accurate and cost-effective alternative method for measuring cell migration with the circular wound closure assay.* Bioscience Reports, 2018. **38**(5): p. BSR20180698.
111. Jonkman, J.E.N., J.A. Cathcart, F. Xu, M.E. Bartolini, J.E. Amon, K.M. Stevens and P. Colarusso, *An introduction to the wound healing assay using live-cell microscopy.* Cell Adhesion & Migration, 2014. **8**(5): p. 440-451.
112. Lv, X., Z. Geng, Z. Fan, S. Wang, W. Pei and H. Chen, *A PDMS Device Coupled with Culture Dish for In Vitro Cell Migration Assay.* Applied Biochemistry and Biotechnology, 2018. **186**(3): p. 633-643.
113. Xu, J., X. Wang, X. Li, G. Yang and C. Luo *High-throughput cell migration assay under combinatorial chemical environments by a novel 24-well-plate based device*. Biomedical microdevices, 2020. **22**, 40 DOI: 10.1007/s10544-020-00491-7.
114. Veres-Székely, A., D. Pap, B. Szebeni, L. Őrfi, C. Szász, C. Pajtók, E. Lévai, A.J. Szabó and Á. Vannay, *Transient Agarose Spot (TAS) Assay: A New Method to Investigate Cell Migration.* International Journal of Molecular Sciences, 2022. **23**(4).

115. 2022.06.03.]; Available from: https://pubmed.ncbi.nlm.nih.gov/?term=scratch+assay&sort=date.
116. Kemeny, L.V., Z. Kurgyis, T. Buknicz, G. Groma, A. Jakab, K. Zanker, T. Dittmar, L. Kemeny and I.B. Nemeth, *Melanoma Cells Can Adopt the Phenotype of Stromal Fibroblasts and Macrophages by Spontaneous Cell Fusion in Vitro.* Int J Mol Sci, 2016. **17**(6).
117. Veres-Székely, A., D. Pap, E. Sziksz, E. Jávorszky, R. Rokonay, R. Lippai, K. Tory, A. Fekete, T. Tulassay, A.J. Szabó and Á. Vannay, *Selective measurement of α smooth muscle actin: why β-actin can not be used as a housekeeping gene when tissue fibrosis occurs.* BMC Mol Biol., 2017(1471-2199).
118. Korzeniewski, C. and D.M. Callewaert, *An enzyme-release assay for natural cytotoxicity*. Journal of Immunological Methods, 1983. **64**(3): p. 313-320.
119. Mosmann, T., *Rapid colorimetric assay for cellular growth and survival: Application to proliferation and cytotoxicity assays.* Journal of Immunological Methods, 1983. **65**(1): p. 55-63.
120. Walsh, B.J., R. Thornton Sc Fau - Penny, S.N. Penny R Fau - Breit and S.N. Breit, *Microplate reader-based quantitation of collagens.* Anal Biochem., 1992(0003-2697).
121. Faraco, G., D. Brea, L. Garcia-Bonilla, G. Wang, G. Racchumi, H. Chang, I. Buendia, M.M. Santisteban, S.G. Segarra, K. Koizumi, Y. Sugiyama, M. Murphy, H. Voss, J. Anrather and C. Iadecola, *Dietary salt promotes neurovascular and cognitive dysfunction through a gut-initiated TH17 response.* Nature Neuroscience, 2018. **21**(2): p. 240-249.
122. Ferguson, J.F., L.A. Aden, N.R. Barbaro, J.P. Van Beusecum, L. Xiao, A.J. Simmons, C. Warden, L. Pasic, L.E. Himmel, M.K. Washington, F.L. Revetta, S. Zhao, S. Kumaresan, M.B. Scholz, Z. Tang, G. Chen, M.P. Reilly and A. Kirabo, *High dietary salt–induced DC activation underlies microbial dysbiosis-associated hypertension.* JCI Insight, 2019. **4**(13).
123. Guo, C.-P., Z. Wei, F. Huang, M. Qin, X. Li, Y.-M. Wang, Q. Wang, J.-Z. Wang, R. Liu, B. Zhang, H.-L. Li and X.-C. Wang, *High salt induced hypertension leads to cognitive defect.* Oncotarget, 2017. **8**(56): p. 95780-95790.
124. Cannon, W.B., *The wisdom of the body*. 1932: W. W. Norton & Company.

125. Titze, J., K. Bauer, M. Schafflhuber, P. Dietsch, R. Lang, K.H. Schwind, F.C. Luft, K.-U. Eckardt and K.F. Hilgers, *Internal sodium balance in DOCA-salt rats: a body composition study.* American Journal of Physiology-Renal Physiology, 2005. **289**(4): p. F793-F802.

126. Kopp, C., L. Linz P Fau - Wachsmuth, A. Wachsmuth L Fau - Dahlmann, T. Dahlmann A Fau - Horbach, C. Horbach T Fau - Schöfl, W. Schöfl C Fau - Renz, D. Renz W Fau - Santoro, T. Santoro D Fau - Niendorf, D.N. Niendorf T Fau - Müller, M. Müller Dn Fau - Neininger, A. Neininger M Fau - Cavallaro, K.-U. Cavallaro A Fau - Eckardt, R.E. Eckardt Ku Fau - Schmieder, F.C. Schmieder Re Fau - Luft, M. Luft Fc Fau - Uder, J. Uder M Fau - Titze and J. Titze, *(23)Na magnetic resonance imaging of tissue sodium.* Hypertension., 2012(1524-4563).

127. Schneider, M.P., U. Raff, C. Kopp, J.B. Scheppach, S. Toncar, C. Wanner, G. Schlieper, T. Saritas, J. Floege, M. Schmid, A. Birukov, A. Dahlmann, P. Linz, R. Janka, M. Uder, R.E. Schmieder, J.M. Titze and K.U. Eckardt, *Skin Sodium Concentration Correlates with Left Ventricular Hypertrophy in CKD.* (1533-3450 (Electronic)).

128. Linz, P., D. Santoro, W. Renz, J. Rieger, A. Ruehle, J. Ruff, M. Deimling, N. Rakova, D.N. Muller, F.C. Luft, J. Titze and T. Niendorf, *Skin sodium measured with 23Na MRI at 7.0 T.* NMR in Biomedicine, 2015. **28**(1): p. 54-62.

129. Tubbs, A.L., B. Liu, T.D. Rogers, R.B. Sartor and E.A.-O. Miao, *Dietary Salt Exacerbates Experimental Colitis.* J Immunol., 2017(1550-6606).

130. Wilck, N., M.G. Matus, S.M. Kearney, S.W. Olesen, K. Forslund, H. Bartolomaeus, S. Haase, A. Mähler, A. Balogh, L. Markó, O. Vvedenskaya, F.H. Kleiner, D. Tsvetkov, L. Klug, P.I. Costea, S. Sunagawa, L. Maier, N. Rakova, V. Schatz, P. Neubert, C. Frätzer, A. Krannich, M. Gollasch, D.A. Grohme, B.F. Côrte-Real, R.G. Gerlach, M. Basic, A. Typas, C. Wu, J.M. Titze, J. Jantsch, M. Boschmann, R. Dechend, M. Kleinewietfeld, S. Kempa, P. Bork, R.A. Linker, E.J. Alm and D.N. Müller, *Salt-responsive gut commensal modulates T(H)17 axis and disease.* Nature., 2017(1476-4687).

131. Headland, S.E. and L.V. Norling, *The resolution of inflammation: Principles and challenges.* Seminars in Immunology, 2015. **27**(3): p. 149-160.

132. Hutchins, A.P., D. Diez and D. Miranda-Saavedra, *The IL-10/STAT3-mediated anti-inflammatory response: recent developments and future challenges.* Briefings in Functional Genomics, 2013. **12**(6): p. 489-498.

133. King, A., S. Balaji, L.D. Le, T.M. Crombleholme and S.G. Keswani, *Regenerative Wound Healing: The Role of Interleukin-10.* Advances in wound care, 2014. **3**(4): p. 315-323.

134. Cardilo-Reis, L., S. Gruber, S.M. Schreier, M. Drechsler, N. Papac-Milicevic, C. Weber, O. Wagner, H. Stangl, O. Soehnlein and C.J. Binder, *Interleukin-13 protects from atherosclerosis and modulates plaque composition by skewing the macrophage phenotype.* EMBO molecular medicine, 2012. **4**(10): p. 1072-1086.

135. Kolosowska, N., M.H. Keuters, S. Wojciechowski, V. Keksa-Goldsteine, M. Laine, T. Malm, G. Goldsteins, J. Koistinaho and H.A.-O. Dhungana, *Peripheral Administration of IL-13 Induces Anti-inflammatory Microglial/Macrophage Responses and Provides Neuroprotection in Ischemic Stroke.* Neurotherapeutics., 2019(1878-7479).

136. Noll, J., E. Helk, H. Fehling, H. Bernin, C. Marggraff, T. Jacobs, S. Huber, P. Pelczar, T. Ernst, H. Ittrich, B. Otto, H.W. Mittrücker, C. Hölscher, F. Tacke, I. Bruchhaus, E. Tannich and H. Lotter, *IL-23 prevents IL-13-dependent tissue repair associated with Ly6C(lo) monocytes in Entamoeba histolytica-induced liver damage.* J Hepatol., 2016(1600-0641).

137. Saraiva, M. and A. O'Garra, *The regulation of IL-10 production by immune cells.* Nat Rev Immunol., 2010(1474-1741).

138. Venkayya, R., M. Lam M Fau - Willkom, G. Willkom M Fau - Grünig, D.B. Grünig G Fau - Corry, D.J. Corry Db Fau - Erle and D.J. Erle, *The Th2 lymphocyte products IL-4 and IL-13 rapidly induce airway hyperresponsiveness through direct effects on resident airway cells.* Am J Respir Cell Mol Biol., 2002(1044-1549).

139. Pfisterer, K., L.E. Shaw, D. Symmank and W. Weninger, *The Extracellular Matrix in Skin Inflammation and Infection.* Frontiers in Cell and Developmental Biology, 2021. **9**.

140. Tracy, L.E., R.A. Minasian and E.J. Caterson, *Extracellular Matrix and Dermal Fibroblast Function in the Healing Wound.* Advances in wound care, 2016. **5**(3): p. 119-136.

141. Chadli, L., B. Sotthewes, K. Li, S.N. Andersen, E. Cahir-McFarland, M. Cheung, P. Cullen, A. Dorjée, J.K. de Vries-Bouwstra, T.W.J. Huizinga, D.F. Fischer, J. DeGroot, J.L. Viney, T.S. Zheng, J. Aarbiou and A. Gardet, *Identification of regulators of the myofibroblast phenotype of primary dermal fibroblasts from early diffuse systemic sclerosis patients.* Scientific reports, 2019. **9**(1): p. 4521-4521.

142. Hinz, B., G. Celetta, J.J. Tomasek, G. Gabbiani and C. Chaponnier, *Alpha-Smooth Muscle Actin Expression Upregulates Fibroblast Contractile Activity.* Molecular Biology of the Cell, 2001. **12**(9): p. 2730-2741.

143. Pierce, G.F., J. Mustoe Ta Fau - Lingelbach, V.R. Lingelbach J Fau - Masakowski, G.L. Masakowski Vr Fau - Griffin, R.M. Griffin Gl Fau - Senior, T.F. Senior Rm Fau - Deuel and T.F. Deuel, *Platelet-derived growth factor and transforming growth factor-beta enhance tissue repair activities by unique mechanisms.* J Cell Biol., 1989(0021-9525).

144. Shook, B.A., R.R. Wasko, G.C. Rivera-Gonzalez, E. Salazar-Gatzimas, F. López-Giráldez, B.C. Dash, A.R. Muñoz-Rojas, K.D. Aultman, R.K. Zwick, V. Lei, J.L. Arbiser, K. Miller-Jensen, D.A. Clark, H.C. Hsia and V. Horsley, *Myofibroblast proliferation and heterogeneity are supported by macrophages during skin repair.* Science, 2018. **362**(6417): p. eaar2971.

145. Heldin, C.H. and B. Westermark, *Mechanism of action and in vivo role of platelet-derived growth factor.* Physiol Rev., 1999(0031-9333).

146. Martinet Y Fau - Bitterman, P.B., J.F. Bitterman Pb Fau - Mornex, G.R. Mornex Jf Fau - Grotendorst, G.R. Grotendorst Gr Fau - Martin, R.G. Martin Gr Fau - Crystal and R.G. Crystal, *Activated human monocytes express the c-sis proto-oncogene and release a mediator showing PDGF-like activity.* Nature., 1986(0028-0836).

147. D'Arpino, M.C., A.G. Fuchs, S.S. Sánchez and S.M. Honoré, *Extracellular matrix remodeling and TGF-β1/Smad signaling in diabetic colon mucosa.* Cell Biology International, 2018. **42**(4): p. 443-456.

148. Hao, J., H. Ju, S. Zhao, A. Junaid, T. Scammell-La Fleur and I.M.C. Dixon, *Elevation of Expression of Smads 2, 3, and 4, Decorin and TGF-βin the Chronic Phase of Myocardial Infarct Scar Healing.* Journal of Molecular and Cellular Cardiology, 1999. **31**(3): p. 667-678.

149. Liu, Y., C. Meyer, A. Müller, F. Herweck, Q. Li, R. Müllenbach, P.R. Mertens, S. Dooley and H.-L. Weng, *IL-13 Induces Connective Tissue Growth Factor in Rat Hepatic Stellate Cells via TGF-β–Independent Smad Signaling.* The Journal of Immunology, 2011. **187**(5): p. 2814.

150. Nguyen, J.K., E. Austin, A. Huang, A. Mamalis and J. Jagdeo, *The IL-4/IL-13 axis in skin fibrosis and scarring: mechanistic concepts and therapeutic targets.* Archives of Dermatological Research, 2020. **312**(2): p. 81-92.

151. Zhou, X., H. Hu, M.-L.N. Huynh, C. Kotaru, S. Balzar, J.B. Trudeau and S.E. Wenzel, *Mechanisms of tissue inhibitor of metalloproteinase 1 augmentation by IL-13 on TGF-β1–stimulated primary human fibroblasts.* Journal of Allergy and Clinical Immunology, 2007. **119**(6): p. 1388-1397.

152. Derynck, R. and Y.E. Zhang, *Smad-dependent and Smad-independent pathways in TGF-β family signalling.* Nature, 2003. **425**(6958): p. 577-584.

153. Jinnin, M., K. Ihn H Fau - Yamane, K. Yamane K Fau - Tamaki and K. Tamaki, *Interleukin-13 stimulates the transcription of the human alpha2(I) collagen gene in human dermal fibroblasts.* J Biol Chem., 2004(0021-9258).

154. Oriente, A., S.E. Fedarko Ns Fau - Pacocha, S.K. Pacocha Se Fau - Huang, L.M. Huang Sk Fau - Lichtenstein, D.M. Lichtenstein Lm Fau - Essayan and D.M. Essayan, *Interleukin-13 modulates collagen homeostasis in human skin and keloid fibroblasts.* J Pharmacol Exp Ther., 2000(0022-3565).

155. Martin, P., W.R. Teodoro, A.P.P. Velosa, J. de Morais, S. Carrasco, R.B. Christmann, C. Goldenstein-Schainberg, E.R. Parra, M.L. Katayama, M.N. Sotto, V.L. Capelozzi and N.H. Yoshinari, *Abnormal collagen V deposition in dermis correlates with skin thickening and disease activity in systemic sclerosis.* Autoimmunity Reviews, 2012. **11**(11): p. 827-835.

156. Oyoshi, M.K., R. He, Y. Kanaoka, A. ElKhal, S. Kawamoto, C.N. Lewis, K.F. Austen and R.S. Geha, *Eosinophil-derived leukotriene C4 signals via type 2 cysteinyl leukotriene receptor to promote skin fibrosis in a mouse model of atopic*

dermatitis. Proceedings of the National Academy of Sciences, 2012. **109**(13): p. 4992.

157. Smith, G.P. and E.S.L. Chan, *Molecular pathogenesis of skin fibrosis: insight from animal models.* Current rheumatology reports, 2010. **12**(1): p. 26-33.

158. Stamenkovic, I., *Extracellular matrix remodelling: the role of matrix metalloproteinases.* J Pathol., 2003(0022-3417 (Print)).

159. Lafuma, C., R.A. El Nabout, F. Crechet, A. Hovnanian and M. Martin, *Expression of 72-kDa Gelatinase (MMP-2), Collagenase (MMP-1), and Tissue Metalloproteinase Inhibitor (TIMP) in Primary Pig Skin Fibroblast Cultures Derived from Radiation-Induced Skin Fibrosis.* Journal of Investigative Dermatology, 1994. **102**(6): p. 945-950.

160. Madlener, M., W.C. Parks and S. Werner, *Matrix Metalloproteinases (MMPs) and Their Physiological Inhibitors (TIMPs) Are Differentially Expressed during Excisional Skin Wound Repair.* Experimental Cell Research, 1998. **242**(1): p. 201-210.

161. Davidson, B., J. Goldberg I Fau - Kopolovic, L. Kopolovic J Fau - Lerner-Geva, W.H. Lerner-Geva L Fau - Gotlieb, G. Gotlieb Wh Fau - Ben-Baruch, R. Ben-Baruch G Fau - Reich and R. Reich, *MMP-2 and TIMP-2 expression correlates with poor prognosis in cervical carcinoma--a clinicopathologic study using immunohistochemistry and mRNA in situ hybridization.* Gynecologic Oncology, 1999(0090-8258 (Print)).

162. Grzela, T., J. Niderla-Bielinska, M. Litwiniuk and R. White, *The direct inhibition of MMP-2 and MMP-9 by an enzyme alginogel: a possible mechanism of healing support for venous leg ulcers.* Journal of Wound Care, 2014(0969-0700 (Print)).

163. Serra, R., G. Buffone, D. Falcone, V. Molinari, M. Scaramuzzino, L. Gallelli and S. de Franciscis, *Chronic venous leg ulcers are associated with high levels of metalloproteinases-9 and neutrophil gelatinase-associated lipocalin.* Wound Repair and Regeneration, 2013. **21**(3): p. 395-401.

164. Al-Khafaji, F., M. Wiltshire, D. Fuhrer, G. Mazziotti, M.D. Lewis, P.J. Smith and M. Ludgate, *Biological activity of activating thyrotrophin receptor mutants: modulation by iodide.* Journal of Molecular Endocrinology, 2005. **34**(1): p. 209-220.

165. Kawakami, Y., S. Imran, M. Katsuhara and Y. Tada, *Na+ Transporter SvHKT1;1 from a Halophytic Turf Grass Is Specifically Upregulated by High Na+ Concentration and Regulates Shoot Na+ Concentration.* International Journal of Molecular Sciences, 2020. **21**(17).

166. Mogilner, A. and K. Keren, *The shape of motile cells.* Current biology : CB, 2009. **19**(17): p. R762-R771.

167. Bershadsky, A.D., T.M. Tint Is Fau - Svitkina and T.M. Svitkina, *Association of intermediate filaments with vinculin-containing adhesion plaques of fibroblasts.* Cell Motil Cytoskeleton., 1987(0886-1544).

168. Bunnell, T.M., Y. Burbach Bj Fau - Shimizu, J.M. Shimizu Y Fau - Ervasti and J.M. Ervasti, *β-Actin specifically controls cell growth, migration, and the G-actin pool.* Mol Biol Cell., 2011(1939-4586).

169. Gao, L.R., G. Wang, J. Zhang, S. Li, M. Chuai, Y. Bao, B. Hocher and X.A.-O. Yang, *High salt-induced excess reactive oxygen species production resulted in heart tube malformation during gastrulation.* J Cell Physiol., 2018(1097-4652).

170. Torres, B.M., M.A.S. Leal, B.F. Brun, M.L. Porto, S.F.S. Melo, E.M. de Oliveira, V.G. Barauna and P.F. Vassallo, *Effects of direct high sodium exposure at endothelial cell migration.* Biochem Biophys Res Commun., 2019(1090-2104).

171. Zhao, J., B. Shu, L. Chen, J. Tang, L. Zhang, J. Xie, X. Liu, Y. Xu and S. Qi, *Prostaglandin E2 inhibits collagen synthesis in dermal fibroblasts and prevents hypertrophic scar formation in vivo.* Exp Dermatol., 2016(1600-0625).

172. Kim, D., S.Y. Kim, S.K. Mun, S. Rhee and B.J. Kim, *Epidermal growth factor improves the migration and contractility of aged fibroblasts cultured on 3D collagen matrices.* Int J Mol Med, 2015. **35**(4): p. 1017-1025.

173. Yu, A., Y. Matsuda, A. Takeda, E. Uchinuma and Y. Kuroyanagi, *Effect of EGF and bFGF on Fibroblast Proliferation and Angiogenic Cytokine Production from Cultured Dermal Substitutes.* Journal of Biomaterials Science, Polymer Edition, 2012. **23**(10): p. 1315-1324.

174. Liang, C.-C., A.Y. Park and J.-L. Guan, *In vitro scratch assay: a convenient and inexpensive method for analysis of cell migration in vitro.* Nature Protocols, 2007. **2**(2): p. 329-333.

175. Kam, Y., C. Guess, L. Estrada, B. Weidow and V. Quaranta, *A novel circular invasion assay mimics in vivo invasive behavior of cancer cell lines and distinguishes single-cell motility in vitro.* BMC Cancer, 2008. **8**(1): p. 198.
176. Stamm, A., K. Reimers, S. Strauß, P. Vogt, T. Scheper and I. Pepelanova, *In vitro wound healing assays – state of the art.* BioNanoMaterials, 2016. **17**(1-2): p. 79-87.
177. Salati, M.A., J. Khazai, A.M. Tahmuri, A. Samadi, A. Taghizadeh, M. Taghizadeh, P. Zarrintaj, J.D. Ramsey, S. Habibzadeh, F. Seidi, M.R. Saeb and M. Mozafari, *Agarose-Based Biomaterials: Opportunities and Challenges in Cartilage Tissue Engineering.* Polymers, 2020. **12**(5).
178. Zarrintaj, P., S. Manouchehri, Z. Ahmadi, M.R. Saeb, A.M. Urbanska, D.L. Kaplan and M. Mozafari, *Agarose-based biomaterials for tissue engineering.* Carbohydrate Polymers, 2018. **187**: p. 66-84.
179. Ware, M.F., A. Wells and D.A. Lauffenburger, *Epidermal growth factor alters fibroblast migration speed and directional persistence reciprocally and in a matrix-dependent manner.* Journal of Cell Science, 1998. **111**(16): p. 2423-2432.
180. Yu, J., A. Moon and H.-R.C. Kim, *Both Platelet-Derived Growth Factor Receptor (PDGFR)-α and PDGFR-β Promote Murine Fibroblast Cell Migration.* Biochemical and Biophysical Research Communications, 2001. **282**(3): p. 697-700.

9. Bibliography of the candidate's publications

9.1. Research articles related to the theme of the PhD thesis

- Pajtók C, Veres-Székely A, Agócs R, Szebeni B, Dobosy P, Németh I, Veréb Z, Kemény L, Szabó AJ, Vannay Á, Tulassay T, Pap D. (2021) High salt diet impairs dermal tissue remodeling in a mouse model of IMQ induced dermatitis. PLOS ONE 16(11): e0258502. https://doi.org/10.1371/journal.pone.0258502
- Veres-Székely A, Pap D, Szebeni B, Őrfi L, Szász C, Pajtók C, Lévai E, Szabó AJ, Vannay Á. (2022) Transient Agarose Spot (TAS) Assay: A New Method to Investigate Cell Migration. International Journal of Molecular Sciences 23(4):2119. https://doi.org/10.3390/ijms23042119

9.2. Other publications

- Becsei D*, Pajtók Cs*, Körner A, Szabó AJ. (2020) A COVID-19 gyermekgyógyászati vonatkozásai: Pediatric aspects of COVID-19. ORVOSKÉPZÉS 95 : 3 pp. 532-538. , 7 p. *Equally contributed
- Szalai Zs, Bánki D, Pajtók Cs (2023) A mikrobiális flóra jelentősége atopiás dermatitisben – áttekintés. Gyermekgyógyászat. ISSN: 0017-5900

10. Acknowledgements

I am grateful to my supervisor, Dr. Domonkos Pap, for his invaluable patience and time for shaping my research approach.

I would like to express my sincere thanks to Dr Ádám Vannay and Professor Tivadar Tulassay, who have helped me throughout my work with his knowledge, experience and feedback.

I am also grateful to Professor Attila Szabó for the opportunity to carry out my research within the framework provided by the Research Laboratory of the 1st Department of Pediatrics of Semmelweis University.

I am also thankful for the help of the Research Laboratory of the 1st Department of Pediatrics and all the staff of the ELKH-SE Paediatric and Nephrology Research Group, emphasizing the motivating attitude and selfless support of Dr. Eszter Lévai, Dr. Apor Veres-Székely, Dr. Beáta Szebeni, Mária Bernáth, Tamás Lakat and Ákos Tóth.

Last but not least, I am deeply indebted to my fiancé, Dr. Tamás Nádasy, and my family for their emotional support and endless encouragement.